must be overcome before effective PTD-based drug delivery carriers can be fully developed. We previously reported that cotreatment with HA2-Tat enhances the cytosolic release of Tat-fused peptide-blockers and their biological activities, thereby overcoming the issue of endosome entrapment (Sugita *et al.*, 2007). Furthermore, although the transduction mechanism of PTDs is not yet well understood, these differences led us to explore the possibility of creating novel PTDs. We successfully created novel PTDs that have higher transduction efficiencies than Tat, using a unique phage display-based screening strategy that we previously developed (Mukai *et al.*, 2006; Kamada *et al.*, 2007). Moreover, based on our PTD-screening system, we are currently working to create more useful PTDs with cell type specificity.

Conflict of interest

The authors state no conflict of interest.

References

Berlose JP, Convert O, Derossi D, Brunissen A, Chassaing G (1996). Conformational and associative behaviours of the third helix of antennapedia homeodomain in membrane-mimetic environments. *Eur J Biochem* **242**: 372–386.

Borsello T, Forloni G (2007). JNK signalling: a possible target to prevent neurodegeneration. *Curr Pharm Des* **13**: 1875–1886.

Brusic V, Marina O, Wu CJ, Reinherz EL (2007). Proteome informatics for cancer research: from molecules to clinic. *Proteomics* **7**: 976–991.

Chauhan A, Tikoo A, Kapur AK, Singh M (2007). The taming of the cell penetrating domain of the HIV Tat: myths and realities. *J Control Release* **117**: 148–162.

Console S, Marty C, Garcia-Echeverria C, Schwendener R, Ballmer-Hofer K (2003). Antennapedia and HIV transactivator of transcription (TAT) 'protein transduction domains' promote endocytosis of high molecular weight cargo upon binding to cell surface glycosaminoglycans. *J Biol Chem* **278**: 35109–35114.

Derossi D, Joliot AH, Chassaing G, Prochiantz A (1994). The third helix of the Antennapedia homeodomain translocates through biological membranes. *J Biol Chem* **269**: 10444–10450.

Drabik A, Bierczynska-Krzysik A, Bodzon-Kulakowska A, Suder P, Kotlinska J, Silberring J (2007). Proteomics in neurosciences. *Mass Spectrom Rev* **26**: 432–450.

El-Andaloussi S, Jarver P, Johansson HJ, Langel U (2007). Cargo dependent cytotoxicity and delivery efficacy of cell-penetrating peptides: a comparative study. *Biochem J* **407**: 285–292.

Elliott G, O'Hare P (1997). Intercellular trafficking and protein delivery by a herpesvirus structural protein. *Cell* **88**: 223–233.

Ferrari A, Pellegrini V, Arcangeli C, Fittipaldi A, Giacca M, Beltram F (2003). Caveolae-mediated internalization of extracellular HIV-1 tat fusion proteins visualized in real time. *Mol Ther* **8**: 284–294.

Fittipaldi A, Ferrari A, Zoppe M, Arcangeli C, Pellegrini V, Beltram F *et al.* (2003). Cell membrane lipid rafts mediate caveolar endocytosis of HIV-1 Tat fusion proteins. *J Biol Chem* **278**: 34141–34149.

Futaki S, Suzuki T, Ohashi W, Yagami T, Tanaka S, Ueda K *et al.* (2001). Arginine-rich peptides. An abundant source of membrane-permeable peptides having potential as carriers for intracellular protein delivery. *J Biol Chem* **276**: 5836–5840.

Grimmer S, van Deurs B, Sandvig K (2002). Membrane ruffling and macropinocytosis in A431 cells require cholesterol. *J Cell Sci* **115**: 2953–2962.

Hallbrink M, Floren A, Elmquist A, Pooga M, Bartfai T, Langel U (2001). Cargo delivery kinetics of cell-penetrating peptides. *Biochim Biophys Acta* **1515**: 101–109.

Han X, Bushweller JH, Cafiso DS, Tamm LK (2001). Membrane structure and fusion-triggering conformational change of the fusion domain from influenza hemagglutinin. *Nat Struct Biol* **8**: 715–720.

Hawiger J (1999). Noninvasive intracellular delivery of functional peptides and proteins. *Curr Opin Chem Biol* **3**: 89–94.

Joliot A, Prochiantz A (2004). Transduction peptides: from technology to physiology. *Nat Cell Biol* **6**: 189–196.

Jones SW, Christison R, Bundell K, Voyce CJ, Brockbank SM, Newham P *et al.* (2005). Characterisation of cell-penetrating peptide-mediated peptide delivery. *Br J Pharmacol* **145**: 1093–1102.

Kamada H, Okamoto T, Kawamura M, Shibata H, Abe Y, Ohkawa A *et al.* (2007). Creation of novel cell-penetrating peptides for intracellular drug delivery using systematic phage display technology originated from Tat transduction domain. *Biol Pharm Bull* **30**: 218–223.

Kaplan IM, Wadia JS, Dowdy SF (2005). Cationic TAT peptide transduction domain enters cells by macropinocytosis. *J Control Release* **102**: 247–253.

Liu NQ, Lossinsky AS, Popik W, Li X, Gujuluva C, Kriederman B *et al.* (2002). Human immunodeficiency virus type 1 enters brain microvascular endothelia by macropinocytosis dependent on lipid rafts and the mitogen-activated protein kinase signaling pathway. *J Virol* **76**: 6689–6700.

Lundberg M, Wikstrom S, Johansson M (2003). Cell surface adherence and endocytosis of protein transduction domains. *Mol Ther* **8**: 143–150.

Mukai Y, Sugita T, Yamato T, Yamanada N, Shibata H, Imai S *et al.* (2006). Creation of novel protein transduction domain (PTD) mutants by a phage display-based high-throughput screening system. *Biol Pharm Bull* **29**: 1570–1574.

Murriel CL, Dowdy SF (2006). Influence of protein transduction domains on intracellular delivery of macromolecules. *Expert Opin Drug Deliv* **3**: 739–746.

Nagahara H, Vocero-Akbani AM, Snyder EL, Ho A, Latham DG, Lissy NA *et al.* (1998). Transduction of full-length TAT fusion proteins into mammalian cells: TAT-p27Kip1 induces cell migration. *Nat Med* **4**: 1449–1452.

Nori A, Kopecek J (2005). Intracellular targeting of polymer-bound drugs for cancer chemotherapy. *Adv Drug Deliv Rev* **57**: 609–636.

Pujals S, Fernandez-Carneado J, Lopez-Iglesias C, Kogan MJ, Giralt E (2006). Mechanistic aspects of CPP-mediated intracellular drug delivery: relevance of CPP self-assembly. *Biochim Biophys Acta* **1758**: 264–279.

Rhodes DR, Chinnaiyan AM (2005). Integrative analysis of the cancer transcriptome. *Nat Genet* **37** (Suppl): S31–S37.

Richard JP, Melikov K, Brooks H, Prevot P, Lebleu B, Chernomordik LV (2005). Cellular uptake of unconjugated TAT peptide involves clathrin-dependent endocytosis and heparan sulfate receptors. *J Biol Chem* **280**: 15300–15306.

Richard JP, Melikov K, Vives E, Ramos C, Verbeure B, Gait MJ *et al.* (2003). Cell-penetrating peptides. A reevaluation of the mechanism of cellular uptake. *J Biol Chem* **278**: 585–590.

Rojas M, Donahue JP, Tan Z, Lin YZ (1998). Genetic engineering of proteins with cell membrane permeability. *Nat Biotechnol* **16**: 370–375.

Saar K, Lindgren M, Hansen M, Eiriksdottir E, Jiang Y, Rosenthal-Aizman K *et al.* (2005). Cell-penetrating peptides: a comparative membrane toxicity study. *Anal Biochem* **345**: 55–65.

Sampath P, Pollard TD (1991). Effects of cytochalasin, phalloidin, and pH on the elongation of actin filaments. *Biochemistry* **30**: 1973–1980.

Schmid SL (1997). Clathrin-coated vesicle formation and protein sorting: an integrated process. *Annu Rev Biochem* **66**: 511–548.

Schwarze SR, Ho A, Vocero-Akbani A, Dowdy SF (1999). *In vivo* protein transduction: delivery of a biologically active protein into the mouse. *Science* **285**: 1569–1572.

Schwarze SR, Hruska KA, Dowdy SF (2000). Protein transduction: unrestricted delivery into all cells? *Trends Cell Biol* **10**: 290–295.

Skehel JJ, Cross K, Steinhauer D, Wiley DC (2001). Influenza fusion peptides. *Biochem Soc Trans* **29**: 623–626.

Sugita T, Yoshikawa T, Mukai Y, Yamanada N, Imai S, Nagano K *et al.* (2007). Improved cytosolic translocation and tumor-killing

activity of Tat-shepherdin conjugates mediated by co-treatment with Tat-fused endosome-disruptive HA2 peptide. *Biochem Biophys Res Commun* **363**: 1027–1032.

Tyagi M, Rusnati M, Presta M, Giacca M (2001). Internalization of HIV-1 tat requires cell surface heparan sulfate proteoglycans. *J Biol Chem* **276**: 3254–3261.

Wadia JS, Stan RV, Dowdy SF (2004). Transducible TAT-HA fusogenic peptide enhances escape of TAT-fusion proteins after lipid raft macropinocytosis. *Nat Med* **10**: 310–315.

West MA, Bretscher MS, Watts C (1989). Distinct endocytotic pathways in epidermal growth factor-stimulated human carcinoma A431 cells. *J Cell Biol* **109**: 2731–2739.

Yandek LE, Pokorny A, Floren A, Knoelke K, Langel U, Almeida PF (2007). Mechanism of the cell-penetrating peptide transportan 10 permeation of lipid bilayers. *Biophys J* **92**: 2434–2444.

Ziegler A, Seelig J (2004). Interaction of the protein transduction domain of HIV-1 TAT with heparan sulfate: binding mechanism and thermodynamic parameters. *Biophys J* **86**: 254–263.

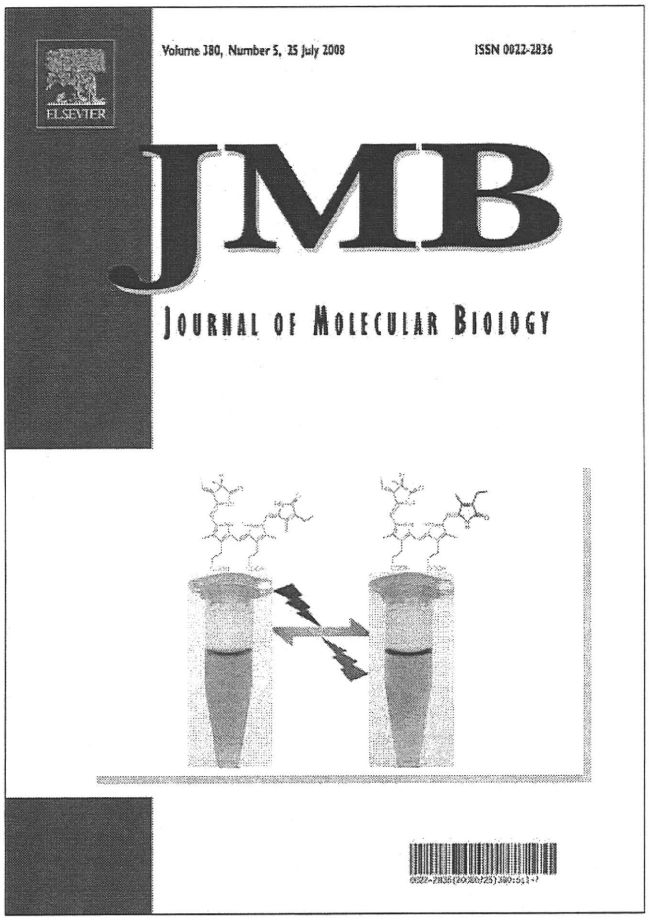

doi:10.1016/j.jmb.2008.05.047 J. Mol. Biol. (2008) 380, 777–782

JMB

Available online at www.sciencedirect.com

ScienceDirect

ELSEVIER

COMMUNICATION

Organelle-Targeted Delivery of Biological Macromolecules Using the Protein Transduction Domain: Potential Applications for Peptide Aptamer Delivery into the Nucleus

Tomoaki Yoshikawa[1,2]†, Toshiki Sugita[1,2]†, Yohei Mukai[1,2], Natsue Yamanada[1,2], Kazuya Nagano[1,2], Hiromi Nabeshi[1,2], Yasuo Yoshioka[1,3], Shinsaku Nakagawa[2], Yasuhiro Abe[1], Haruhiko Kamada[1,3], Shin-ichi Tsunoda[1,3]* and Yasuo Tsutsumi[1,2,3]

[1]*Laboratory of Pharmaceutical Proteomics, National Institute of Biomedical Innovation, 7-6-8 Saito-Asagi, Ibaraki, Osaka 567-0085, Japan*

[2]*Graduate School of Pharmaceutical Sciences, Osaka University, 1-6 Yamadaoka, Suita, Osaka 565-0871, Japan*

[3]*The Center for Advanced Medical Engineering and Informatics, Osaka University, 1-6 Yamadaoka, Suita, Osaka 565-0871, Japan*

Received 5 March 2008; received in revised form 16 May 2008; accepted 21 May 2008
Available online 29 May 2008

Edited by J. Karn

Extensive effort is currently being expended on the innovative design and engineering of new molecular carrier systems for the organelle-targeted delivery of biological cargoes (e.g., peptide aptamers or biological proteins) as tools in cell biology and for developing novel therapeutic approaches. Although cell-permeable Tat peptides are useful carriers for delivering biological molecules into the cell, much internalized Tat-fused cargo is trapped within macropinosomes and thus not delivered into organelles. Here, we devised a novel intracellular targeting technique to deliver Tat-fused cargo into the nucleus using an endosome-disruptive peptide (hemagglutinin-2 subunit) and a nuclear localization signal peptide. We show for the first time that Tat-conjugated peptide aptamers can be selectively delivered to the nucleus by using combined hemagglutinin-2 subunit and nuclear localization signal peptides. This nuclear targeting technique resulted in marked enhancement of the cytostatic activity of a Tat-fused p53-derived peptide aptamer against human MDM2 (mouse double minute 2) that inhibits p53–MDM2 binding. Thus, our technique provides a unique methodology for the development of novel therapeutic approaches based on intracellular targeting.

Keywords: Tat; HA2; nuclear localization signal; intracellular targeting; peptide aptamer

Progress in molecular biological research on intractable diseases such as cancer is steadily increasing our knowledge of the mechanisms of malignant transformation occurring in tumor cells. However, the complexity of biological interactions makes it increasingly difficult to predict gene and protein functions as we proceed from the immediate metabolic pathway to the levels of the cell and organism. Especially at the cellular level, a variety of tools are available to determine protein function and to develop novel therapeutic approaches, including antisense, peptide modulators, proteins and the overexpression of wild-type or dominant-negative proteins. Small peptides might be able to complement these agents because of

T.S. and T.Y. contributed equally to this work.

*Corresponding author. Laboratory of Pharmaceutical Proteomics, National Institute of Biomedical Innovation, 7-6-8 Saito-Asagi, Ibaraki, Osaka 567-0085, Japan.
E-mail address: tsunoda@nibio.go.jp.

† T.S. and T.Y. contributed equally to this work.

Abbreviations used: MDM2, mouse double minute 2; PTD, protein transduction domain; HA2, hemagglutinin-2 subunit; NLS, nuclear localization signal; NLS–VENUS–Tat, VENUS protein with Tat, NLS and His tag; Tat–cargo, Tat-fused cargo; HA2–Tat, Tat-fused endosome-disruptive HA2 peptide; PM10–Tat, Tat-fused PM10; NLS–PM10–

0022-2836/$ - see front matter

their ability to recognize specific protein domains and thus to interfere with enzymatic functions or protein–protein interactions.[1] Furthermore, these peptides, designated "peptide aptamers," seem to be non-genotoxic and useful for adjunct chemotherapy. However, these approaches are often limited by an inability to effectively deliver the agents to the appropriate cellular location.

Because a prerequisite for their intracellular action is their delivery into cells, various intracellular delivery approaches, such as protein transduction technology with protein transduction domains (PTDs; e.g., Tat, Antp, VP22, Rev and so on), are currently undergoing intensive scrutiny.[2,3] However, protein transduction technology using PTDs has some disadvantages, one of which is the accumulation of PTDs or PTD-fused peptides in the endocytic compartment. We and others have reported that the main mechanism of protein transduction is penetration into cells by macropinocytosis and that therefore much of the material taken up remains entrapped in the macropinosomes.[4–7] Another disadvantage is that there is no technique for controlling the intracellular distribution of peptide aptamers such that their effects are extremely limited. For these reasons, it is important that peptide aptamers be delivered directly into specific cellular compartments. Because optimal approaches for overcoming these disadvantages have not yet been developed, high concentrations of PTDs or PTD-fused peptides must still be employed in order for the technology to function effectively.

With this in mind, we focused on developing intracellular targeting technology for peptide aptamers fused with Tat protein basic domain residues 47–57 (YGRKKRRQRRR) from human immunodeficiency virus-1 in the context of cancer therapeutics. We recently reported that survivin-targeted peptide aptamers (shepherdin) linked to the NH_2-terminal domain of the influenza virus hemagglutinin-2 subunit (HA2), which is a pH-dependent fusogenic peptide inducing lysis of membranes at low pH levels,[8,9] are efficiently released from macropinosomes. This approach succeeded in inducing the death of survivin-expressing malignant tumor cells.[10] Based on this previous study, here we devised a novel intracellular targeting technology using HA2 and nuclear localization signal (NLS) peptides for converting peptide aptamers into efficient research tools for cell biology and cancer therapeutics. We established for the first time that Tat-conjugated peptide aptamers can be selectively delivered to the nucleus by combining HA2 and NLS peptides. Furthermore, we evaluated the utility of our nuclear targeting method using p53-derived peptide from the human MDM2 (mouse double minute 2, also termed HDM2 in humans)-binding domain (residues 17–26: designated PM10), which is a peptide inhibitor of p53–MDM2 binding.[11] Recent reports suggested that inhibiting p53–MDM2 binding could reactivate the p53 pathway and induce growth-suppressive effects and cell cycle arrest of tumor cells as well as normal cells possessing wild-type p53.[11–17] Because the interaction of p53 and MDM2 takes place inside the nucleus, nuclear delivery of PM10 may potentiate the cytostatic effect of this agent. Indeed, we found that our nuclear targeting technique employing PTD, HA2 and NLS peptides markedly enhanced PM10-mediated cytostatic effects against A549 (human lung adenocarcinoma) and WI-38 (human embryonic fibroblast, lung-derived cell line) cells. These results indicate that our intracellular targeting techniques can deliver the cargo into the appropriate organelle and provide a unique research tool for cellular biology and the development of novel therapeutic approaches.

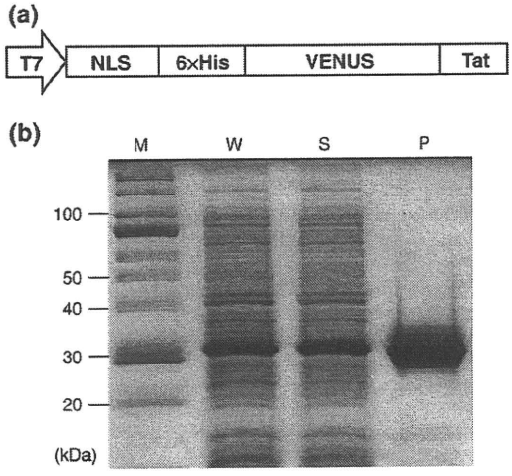

Fig. 1. Vector construction and SDS-PAGE analysis of NLS–VENUS–Tat. (a) Schematic of the NLS–VENUS–Tat region of T7 promoter-driven protein expression vector. The VENUS (variant of yellow fluorescent protein) DNA sequence was kindly provided by Dr. A. Miyawaki (RIKEN Brain Science Institute, Saitama, Japan). The NLS–VENUS–Tat DNA sequence was amplified by PCR. At the 5′ end, the primer sequence 5′-AA CTT TAA GAA GGA GAT ATA *CAT ATG* CCG AAA AAG AAA CGT AAA GTT ACC ATG GCT CAC CAC CAT CAC CAC CAT **GAC TAC AAA GAC GAT GAT GAC AAA** GAA GCT TAC GTG AGC AAG GGC GAG GAG CTG TT-3′ introduced an NdeI site (italics), an NLS (boldface) and a 6× His tag (underline); at the 3′ end, the primer sequence 5′-T TCC TTT CGG GCT TTG TTA GCA GCC *GAA TTC* TTA TTA **ACG GCG ACG CTG GCG ACG TTT TTT ACG ACC GTA** CTC GAG CTT GTA CAG CTC GTC CAT GCC GAG-3′ introduced an EcoRI site (italics) and a Tat sequence (boldface). The PCR product was digested with NdeI as well as EcoRI and inserted into pT7 vector, under the control of the T7 promoter. (b) The plasmid was transformed into *E. coli* BL21 Star (DE3) (Invitrogen, Carlsbad, CA), and cells expressing VENUS proteins were cultured at 25 °C, 250 rpm, for 6 h. The cell paste was then solubilized in a BugBuster Master Mix (Novagen, Darmstadt, Germany) and centrifuged. NLS–VENUS–Tat was recovered in the supernatant and purified by His-tag affinity purification and gel-filtration chromatography. SDS-PAGE analysis was performed under reducing conditions. Lane M, molecular weight standard; lane W, *E. coli* extracts prepared after induction of expression by IPTG; lane S, soluble fractions; lane P, purified proteins.

Tat-fused cargo can be selectively delivered to the nucleus by combining HA2 and NLS peptides

We constructed a VENUS protein (variant of yellow fluorescent protein) fused with Tat, NLS and His tag (NLS–VENUS–Tat) for use as an expression vector (Fig. 1a). NLS–VENUS–Tat was indeed expressed in *Escherichia coli* [BL21 Star (DE3)] after induction with IPTG. The level of expression of the NLS–VENUS–Tat protein was analyzed by SDS-PAGE in total cell lysates (Fig. 1b). Protein expression was specifically induced because we did not find substantially leaky expression of the recombinant protein (data not shown). Recombinant NLS–VENUS–Tat was produced almost entirely in the soluble fraction and had an apparent molecular mass of about 32 kDa under reducing conditions (Fig. 1b, lane S). Purification was carried out by lysis, and separation of the soluble fraction was carried out by centrifugation. This was then loaded onto a Ni^{2+} column for initial purification. The NLS–VENUS–Tat protein eluted from the Ni^{2+} column was more than 90% pure (Fig. 1b, lane P). The purity, apparent molecular mass and cellular internalization activity of the eluted NLS–VENUS–Tat proteins were established by SDS-PAGE and flow cytometry.

Numerous mechanistic studies have shown that Tat peptides rapidly permeate plasma membranes and translocate into the nucleus.[18–22] This mechanism is currently used to deliver proteins and nucleic acids to cell nuclei through covalent linkages of Tat and cargoes.[18] However, nuclear delivery has remained problematic and very limited, because endosome escape and nuclear transport of Tat-fused cargo (Tat–cargo) represent a passive rather than an active process. Indeed, in HeLa cells treated with NLS–VENUS–Tat alone, only punctate cytoplasmic fluorescence, and no fluorescence in the nucleus, was observed (Fig. 2). We had previously confirmed that Tat-fused VENUS co-localized in live cells to vesicles with FM4-64, which is a general endosome marker (data not shown). Furthermore, FAM (carboxyfluorescein) dye-fused Tat peptides also co-localized in FM4-64-positive endosomal vesicles (data not shown). Thus, these results indicated that much of the NLS–VENUS–Tat was entrapped within the endosomal vesicles, resulting in low levels of nuclear accumulation. It is therefore reasonable to propose that Tat–cargo alone cannot reach the targeted cellular compartment, especially the nucleus, and that the therapeutic effects of anticancer peptide aptamers are extremely limited for this reason. Therefore, we devised an active nuclear targeting technique using endosome-disruptive HA2 and SV40-derived NLS peptides.

Recently, we reported that co-treatment with Tat–cargo and the Tat-fused endosome-disruptive HA2 peptide (HA2–Tat) improved the endosome-escape ability and the tumor-killing activity of Tat-fused antisurvivin peptide aptamers.[10] Therefore, we hypothesized that NLS–VENUS–Tat can be delivered into the nucleus if NLS–VENUS–Tat can be engineered to escape from the endosomal vesicles into the cytosol by co-treatment with HA2–Tat. To investigate whether co-treatment with HA2–Tat does effectively improve the nuclear localization of NLS–Tat–cargo, we co-treated HeLa cells with NLS–VENUS–Tat and HA2–Tat and analyzed the intracellular localization of NLS–VENUS–Tat by confocal laser scanning

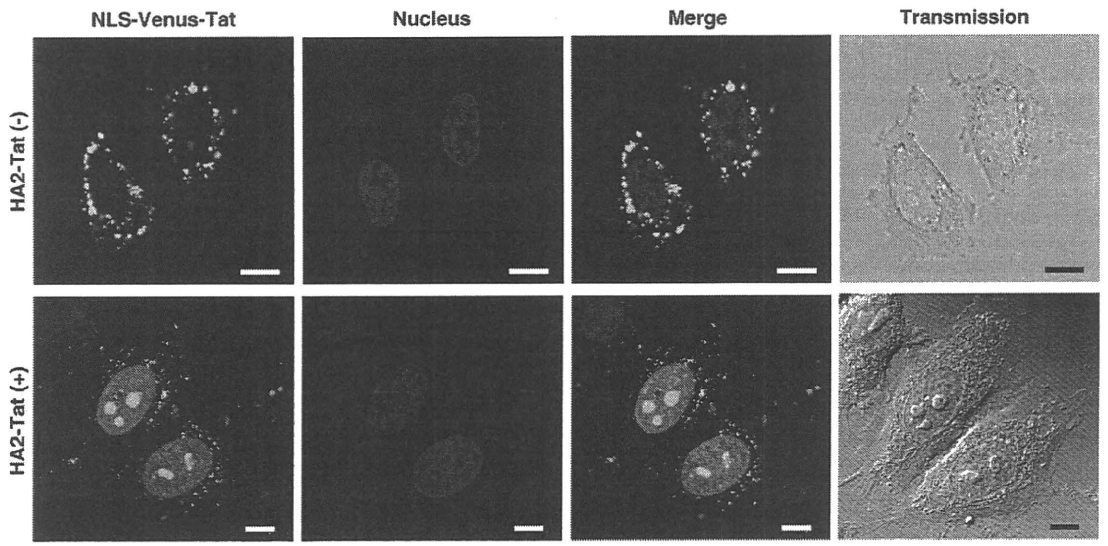

Fig. 2. Intracellular distribution of NLS–VENUS–Tat. HeLa cells were cultured on a Lab-Tek II Chambered Coverglass system (Nalge Nunc International) at 3.0×10^4 cells/well in MEM (minimum essential medium)-α supplemented with 10% fetal bovine serum and incubated for 24 h at 37 °C. Internalization of NLS–VENUS–Tat was performed as follows: HeLa cells were co-treated with NLS–VENUS–Tat (10 μM) with or without HA2–Tat (5 μM) in Opti-MEM I (Invitrogen) containing 100 ng/ml of Hoechst 33342 (Invitrogen). After incubation at 37 °C for 3 h, the medium was changed for a fresh medium and assessed by confocal laser scanning microscopy (Leica Microsystems GmbH, Wetzlar, Germany) without cell fixation. Scale bars in each photomicrograph represent 10 μm.

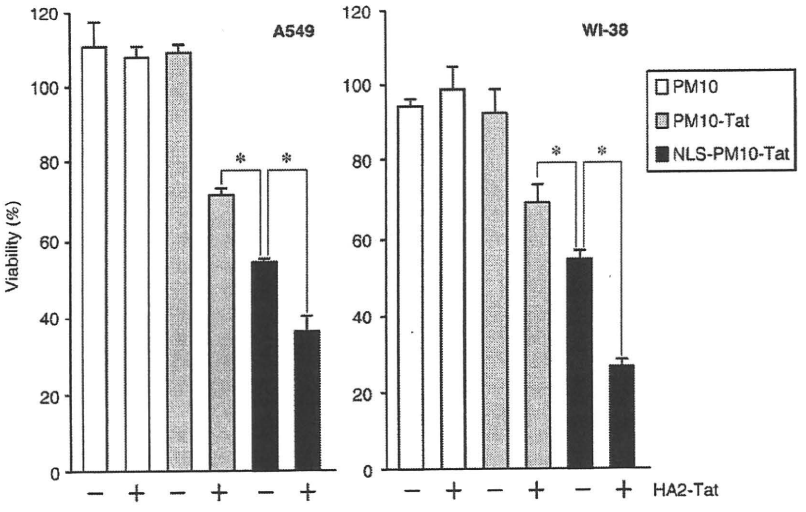

Fig. 3. Nuclear targeting potentiates the cytostatic effect of PM10. All peptides used in this study were purchased from GL Biochem Ltd. (Hiroshima, Japan) with confirmed purities >90% by HPLC and mass spectrography. The sequences of these peptides were GLFEAIEGFIENGWEGMIDGWYG**YGRKKRRQRRR** for HA2–Tat, ETFSDLWKLL for PM10, ETFSDLWKLL**YGRKKRRQRRR** for PM10–Tat and PKKKRKVETFSDLWKLL**YGRKKRRQRRR** for NLS–PM10–Tat. Tat and NLS are shown in boldface and underlined, respectively. A549 or WI-38 cells were seeded into 96-well tissue culture plates (Nalge Nunc International) at 1.0×10^4 cells/well. After incubation for 24 h at 37 °C, the cells were treated with PM10, PM10–Tat or NLS–PM10–Tat at 6 μM (for A549 cells) or 12 μM (for WI-38 cells) in the presence or absence of HA2–Tat (5 μM). After 6 h (for A549 cells) or 24 h (for WI-38 cells), cell viability was determined with the use of WST-8 assay (Nakalai Tesque Inc., Kyoto, Japan) according to the manufacturer's protocol. Data are presented as the mean±SD of triplicate assays. Statistical treatment of the data was performed according to Student's *t* test for two populations (*$p<0.01$).

microscopy (Fig. 2). Co-treatment of HeLa cells with NLS–VENUS–Tat and HA2–Tat resulted in nuclear localization of VENUS, co-localized with Hoechst 33342-stained nuclei. This finding documents that Tat–cargo can be selectively delivered to the nucleus by using HA2 and NLS peptides. Although several groups have attempted to deliver macromolecular drugs to specific organelles, they used PTDs conjugated only with an organelle-targeting signal, such as NLS or mitochondria-targeting signal.[23,24,25] Our data revealed that NLS–VENUS–Tat was entrapped within the endosomal vesicles, with no detectable fluorescence derived from VENUS found in the nucleus. This indicates that organelle targeting by signal-fused PTD–cargo alone does not allow efficient migration into the targeted organelle in the absence of an endosome-escape strategy. Although the influence of the use of different cell types, fluorescent dye, cargo, incubation time and so on could not be excluded as contributing to targeting inability, we found that nuclear transport efficiency could be augmented by combining PTD, HA2 and NLS peptides. Furthermore, our results imply that macromolecules could be delivered into other organelles, such as mitochondria, endoplasmic reticulum and peroxisomes, using different organelle-targeting signal sequences. To this end, we are currently developing novel intracellular drug delivery systems that can target macromolecules into different organelles in a manner analogous to our nuclear targeting techniques.

Nuclear targeting enhances the cytostatic activity of anti-MDM2 peptide aptamer

Next, we tested the utility of our nuclear targeting method using the MDM2-binding peptide aptamer, PM10, which is a p53-derived peptide corresponding to a sequence within the MDM2-binding domain. Kanovsky *et al.* reported that PTD-mediated intracellular delivery of PM10 could reactivate p53 and induce p53-mediated apoptosis of tumor cells with wild-type p53.[11] Under physiological conditions, growth-suppressive and proapoptotic activity of p53 is inhibited by MDM2, which binds p53 and negatively regulates its activity and stability.[16] Recent reports indicated that prevention of p53–MDM2 binding activates the p53 signaling pathway and induces p53-dependent apoptosis in cancer cells possessing wild-type p53.[12,14,15] In addition, the abrogation of p53–MDM2 binding mediates a cytostatic effect and cell cycle arrest in proliferating normal cells.[13,15,17] Because PM10 seems to bind nuclear-localized MDM2 and inhibits MDM2-inducible ubiquitination and degradation of p53, we hypothesized that the nuclear targeting method using HA2 and NLS peptides would enhance its cytotoxicity. To test this, we investigated the effects of treatment with PM10 on cell viability using A549 (human lung adenocarcinoma) and WI-38 (human lung-derived embryonic fibroblast) cells, which possess wild-type p53 (Fig. 3). In A549 and WI-38 cells treated with PM10, Tat-fused PM10 (PM10–Tat) grew vigorously. However, co-treatment with HA2–Tat and PM10–Tat together markedly inhibited A549 and WI-38 cell growth. Furthermore, A549 and WI-38 cells co-treated with HA2–Tat and NLS-fused PM10–Tat (NLS–PM10–Tat) showed greater growth inhibition compared with those treated with NLS–PM10–Tat alone. According to a report from the developers of PM10, although transduction of PTD-fused PM10 (PM10-PTD) into cancer cells could induce tumor cell death *in vitro* and *in vivo*, a high concentration of PM10-PTD was required to see an effect on cancer

cells.[11,26] In contrast, our nuclear targeting technique using PTD, HA2 and NLS peptides markedly enhanced the nuclear localization of the cargo and the PM10-mediated cytostatic effect at low concentrations of PM10. To the best of our knowledge, this is the first report that nuclear targeting of MDM2-binding peptide aptamers can lead to augmentation of cytostatic activity.

In the present study, we aimed to develop a novel cancer therapeutic approach by controlling apoptotic pathways using peptide-based drugs. Recently, the use of intracellular antibodies (intrabodies) directed to a specific target antigen present in the cell has also been suggested as a therapeutic lead to control the apoptotic pathway.[27,28] Our organelle-targeting strategy does seem able to deliver intrabodies directly to the specific organelle in which disease-related proteins reside. Furthermore, we have generated antibodies for various targeted antigens using a non-immune phage scFv library.[29] Thus, we are also currently developing a novel approach to intracellular therapy combining an organelle-targeting strategy and antibody engineering.

Acknowledgements

This study was supported in part by Grants-in-Aid for Scientific Research (20790156) from the Ministry of Education, Culture, Sports, Science and Technology of Japan; in part by a Health and Labor Sciences Research Grant from the Ministry of Health, Labor and Welfare of Japan; in part by a Grant for Industrial Technology Research Program (03A47016a) from the New Energy and Industrial Technology Development Organization of Japan; and in part by funding from the Takeda Science Foundation.

References

1. Mendoza, F. J., Espino, P. S., Cann, K. L., Bristow, N., McCrea, K. & Los, M. (2005). Anti-tumor chemotherapy utilizing peptide-based approaches—apoptotic pathways, kinases, and proteasome as targets. *Arch. Immunol. Ther. Exp.* **53**, 47–60.
2. Dietz, G. P. & Bahr, M. (2004). Delivery of bioactive molecules into the cell: the Trojan horse approach. *Mol. Cell. Neurosci.* **27**, 85–131.
3. Chauhan, A., Tikoo, A., Kapur, A. K. & Singh, M. (2007). The taming of the cell penetrating domain of the HIV Tat: myths and realities. *J. Controlled Release*, **117**, 148–162.
4. Fretz, M., Jin, J., Conibere, R., Penning, N. A., Al-Taei, S., Storm, G. *et al.* (2006). Effects of Na^+/H^+ exchanger inhibitors on subcellular localisation of endocytic organelles and intracellular dynamics of protein transduction domains HIV-TAT peptide and octaarginine. *J. Controlled Release*, **116**, 247–254.
5. Wadia, J. S., Stan, R. V. & Dowdy, S. F. (2004). Transducible TAT-HA fusogenic peptide enhances escape of TAT-fusion proteins after lipid raft macropinocytosis. *Nat. Med.* **10**, 310–315.
6. Sugita, T., Yoshikawa, T., Mukai, Y., Yamanada, N., Imai, S., Nagano, K. *et al.* (2008). Comparative study on transduction and toxicity of protein transduction domains. *Br. J. Pharmacol.* **153**, 1143–1152.
7. Kaplan, I. M., Wadia, J. S. & Dowdy, S. F. (2005). Cationic TAT peptide transduction domain enters cells by macropinocytosis. *J. Controlled Release*, **102**, 247–253.
8. Han, X., Bushweller, J. H., Cafiso, D. S. & Tamm, L. K. (2001). Membrane structure and fusion-triggering conformational change of the fusion domain from influenza hemagglutinin. *Nat. Struct. Biol.* **8**, 715–720.
9. Skehel, J. J., Cross, K., Steinhauer, D. & Wiley, D. C. (2001). Influenza fusion peptides. *Biochem. Soc. Trans.* **29**, 623–626.
10. Sugita, T., Yoshikawa, T., Mukai, Y., Yamanada, N., Imai, S., Nagano, K. *et al.* (2007). Improved cytosolic translocation and tumor-killing activity of Tat-shepherdin conjugates mediated by co-treatment with Tat-fused endosome-disruptive HA2 peptide. *Biochem. Biophys. Res. Commun.* **363**, 1027–1032.
11. Kanovsky, M., Raffo, A., Drew, L., Rosal, R., Do, T., Friedman, F. K. *et al.* (2001). Peptides from the amino terminal mdm-2-binding domain of p53, designed from conformational analysis, are selectively cytotoxic to transformed cells. *Proc. Natl. Acad. Sci. USA*, **98**, 12438–12443.
12. Vassilev, L. T., Vu, B. T., Graves, B., Carvajal, D., Podlaski, F., Filipovic, Z. *et al.* (2004). *In vivo* activation of the p53 pathway by small-molecule antagonists of MDM2. *Science*, **303**, 844–848.
13. Vassilev, L. T. (2004). Small-molecule antagonists of p53–MDM2 binding: research tools and potential therapeutics. *Cell Cycle*, **3**, 419–421.
14. Tovar, C., Rosinski, J., Filipovic, Z., Higgins, B., Kolinsky, K., Hilton, H. *et al.* (2006). Small-molecule MDM2 antagonists reveal aberrant p53 signaling in cancer: implications for therapy. *Proc. Natl. Acad. Sci. USA*, **103**, 1888–1893.
15. Shangary, S., Qin, D., McEachern, D., Liu, M., Miller, R. S., Qiu, S. *et al.* (2008). Temporal activation of p53 by a specific MDM2 inhibitor is selectively toxic to tumors and leads to complete tumor growth inhibition. *Proc. Natl. Acad. Sci. USA*, **105**, 3933–3938.
16. Kubbutat, M. H., Jones, S. N. & Vousden, K. H. (1997). Regulation of p53 stability by Mdm2. *Nature*, **387**, 299–303.
17. Efeyan, A., Ortega-Molina, A., Velasco-Miguel, S., Herranz, D., Vassilev, L. T. & Serrano, M. (2007). Induction of p53-dependent senescence by the MDM2 antagonist nutlin-3a in mouse cells of fibroblast origin. *Cancer Res.* **67**, 7350–7357.
18. Vives, E., Charneau, P., van Rietschoten, J., Rochat, H. & Bahraoui, E. (1994). Effects of the Tat basic domain on human immunodeficiency virus type 1 transactivation, using chemically synthesized Tat protein and Tat peptides. *J. Virol.* **68**, 3343–3353.
19. Vives, E., Brodin, P. & Lebleu, B. (1997). A truncated HIV-1 Tat protein basic domain rapidly translocates through the plasma membrane and accumulates in the cell nucleus. *J. Biol. Chem.* **272**, 16010–16017.
20. Potocky, T. B., Menon, A. K. & Gellman, S. H. (2003). Cytoplasmic and nuclear delivery of a TAT-derived peptide and a beta-peptide after endocytic uptake into HeLa cells. *J. Biol. Chem.* **278**, 50188–50194.
21. Caron, N. J., Quenneville, S. P. & Tremblay, J. P. (2004). Endosome disruption enhances the functional nuclear delivery of Tat-fusion proteins. *Biochem. Biophys. Res. Commun.* **319**, 12–20.

22. Lundberg, M., Wikstrom, S. & Johansson, M. (2003). Cell surface adherence and endocytosis of protein transduction domains. *Mol. Ther.* **8**, 143–150.
23. Shokolenko, I. N., Alexeyev, M. F., LeDoux, S. P. & Wilson, G. L. (2005). TAT-mediated protein transduction and targeted delivery of fusion proteins into mitochondria of breast cancer cells. *DNA Repair (Amst.)*, **4**, 511–518.
24. Del Gaizo, V. & Payne, R. M. (2003). A novel TAT-mitochondrial signal sequence fusion protein is processed, stays in mitochondria, and crosses the placenta. *Mol. Ther.* **7**, 720–730.
25. Matsushita, M., Tomizawa, K., Moriwaki, A., Li, S. T., Terada, H. & Matsui, H. (2001). A high-efficiency protein transduction system demonstrating the role of PKA in long-lasting long-term potentiation. *J. Neurosci.* **21**, 6000–6007.
26. Michl, J., Scharf, B., Schmidt, A., Huynh, C., Hannan, R., von Gizycki, H. *et al.* (2006). PNC-28, a p53-derived peptide that is cytotoxic to cancer cells, blocks pancreatic cancer cell growth *in vivo*. *Int. J. Cancer*, **119**, 1577–1585.
27. Wheeler, Y. Y., Kute, T. E., Willingham, M. C., Chen, S. Y. & Sane, D. C. (2003). Intrabody-based strategies for inhibition of vascular endothelial growth factor receptor-2: effects on apoptosis, cell growth, and angiogenesis. *FASEB J.* **17**, 1733–1735.
28. Williams, B. R. & Zhu, Z. (2006). Intrabody-based approaches to cancer therapy: status and prospects. *Curr. Med. Chem.* **13**, 1473–1480.
29. Imai, S., Mukai, Y., Nagano, K., Shibata, H., Sugita, T., Abe, Y. *et al.* (2006). Quality enhancement of the non-immune phage scFv library to isolate effective antibodies. *Biol. Pharm. Bull.* **29**, 1325–1330.

Hepatoprotective Effect of Syringic Acid and Vanillic Acid on Concanavalin A-Induced Liver Injury

Ayano ITOH,[a] Katsuhiro ISODA,[a] Masuo KONDOH,[a] Masaya KAWASE,[a] Masakazu KOBAYASHI,[b] Makoto TAMESADA,[b] and Kiyohito YAGI*,[a]

[a] *Graduate School of Pharmaceutical Sciences, Osaka University; 1–6 Yamada-oka, Suita, Osaka 565–0871, Japan: and* [b] *Research and Development Center, Kobayashi Pharmaceutical Co., Ltd.; 1–30–3 Toyokawa, Ibaraki, Osaka 567–0057, Japan.* Received December 22, 2008; accepted March 18, 2009; published online April 17, 2009

The edible mushroom *Lentinula edodes* (shiitake) contains many bioactive compounds. In the present study, we cultivated *L. edodes* mycelia in solid medium and examined the hot-water extract (L.E.M.) for its suppressive effect on concanavalin A (ConA)-induced liver injury in mice. ConA injection into the tail vein caused a great increase in the serum aspartate aminotransferase (AST) and alanine aminotransferase (ALT) levels. The intraperitoneal administration of L.E.M. significantly decreased the levels of the transaminases. L.E.M. contains many bioactive substances, including polysaccharides and glucan, which could be immunomodulators. Since ConA-induced liver injury is caused by the activation of T cells, immunomodulating substances might be responsible for the suppressive effect of L.E.M. L.E.M. also contains phenolic compounds that are produced from lignocellulose by mycelia-derived enzymes. The major phenolics in L.E.M., syringic acid and vanillic acid, were intraperitoneally injected into mice shortly before the ConA treatment. Similar to L.E.M., the administration of syringic acid or vanillic acid significantly decreased the transaminase activity and suppressed the disorganization of the hepatic sinusoids. In addition, the inflammatory cytokines tumor necrosis factor (TNF)-α, interferon (IFN)-γ, and interleukin (IL)-6 in the serum increased rapidly, within 3 h of the ConA administration, but the administration of syringic acid or vanillic acid significantly suppressed the cytokine levels. Together, these findings indicate that the phenolic compounds in L.E.M. are hepatoprotective through their suppression of immune-mediated liver inflammation.

Key words hepatoprotection; *Lentinula edodes*; syringic acid; vanillic acid; concanavalin A

Many physiologically active hepatoprotective substances, such as those with antifibrotic activity, have been found in tea, fruits, and vegetables.[1,2] The edible mushroom *Lentinula edodes* (shiitake) contains several bioactive compounds, including compounds with immunoprotective and antiatherogenic activities and one compound with an anti-human immunodeficiency virus (HIV) effect.[3—5] The mycelia of *L. edodes* can be cultured in solid medium, and the extract obtained by hot-water treatment (L.E.M.) is commercially available as a nutritional supplement. In our previous study, we found that L.E.M. exerts a hepatoprotective effect on dimethylnitrosamine (DMN)-induced liver fibrosis and D-galactosamine-induced acute liver injury.[6,7] In the chronic liver injury model that uses DMN, the L.E.M. treatment suppressed the activation of hepatic stellate cells, which play a central role in liver fibrosis. The L.E.M. treatment also protected hepatocytes in the acute liver injury model that uses D-galactosamine. We also found that the oral or intraperitoneal administration of L.E.M. suppressed immune-mediated liver injury. Therefore, L.E.M. is a promising plant extract for the prevention of liver failure. With the aim of developing effective drugs for liver diseases, we examined the protective effect of a single L.E.M. component against liver injury.

The main components of L.E.M. are sugars, proteins, and polyphenolic compounds. The polyphenols act as antioxidants by scavenging reactive oxygen species (ROS), which produce oxidative stress and can adversely affect many cellular processes. Polyphenols have been proposed to protect against several diseases, including cancers, cardiovascular disease, and neurodegenerative disorders.[8—10] In our previous study, we found that the polyphenol-rich fraction of L.E.M. inhibits hepatic stellate cell activation, which is the main cause of liver fibrosis.[6] Among the polyphenols, syringic acid and vanillic acid are enriched in the solid medium of cultured *L. edodes* mycelia. *L. edodes* grown in lignocellulose secretes lignin-degrading peroxidase into the culture medium.[11] The mycelia-derived enzymes degrade the lignin to produce phenolic compounds, particularly syringic acid and vanillic acid. In the present study, we used a mouse model of liver injury to evaluate the hepatoprotective activity of these compounds.

Concanavalin A (ConA)-induced liver injury is a mouse model of immune-mediated liver injury that resembles viral and autoimmune hepatitis in humans.[12] The intravenous injection of ConA into mice increases the plasma alanine aminotransferase (ALT) level; simultaneously, activated T cells infiltrate the liver, and the apoptosis and necrosis of hepatocytes follows. The activation of T cells by ConA results in increased levels of inflammatory cytokines, including tumor necrosis factor (TNF)-α, interferon (IFN)-γ, and interleukin (IL)-6.[13] In the present study, we found that syringic acid and vanillic acid could suppress ConA-induced liver inflammation and damage in mice.

MATERIALS AND METHODS

Animals BALB/c mice were purchased from SLC (Shizuoka, Japan). The animals were housed in an air-conditioned room at 22 °C before the experiment. Hepatic injury was elicited in 6-week-old male mice by injecting ConA (20 mg/kg body weight) (Seikagaku Biobusiness, Tokyo, Japan) into the tail vein. L.E.M., syringic acid (WAKO, Osaka, Japan) or vanillic acid (WAKO, Osaka, Japan) was administered intraperitoneally just before the ConA adminis-

* To whom correspondence should be addressed. e-mail: yagi@phs.osaka-u.ac.jp

tration. L.E.M., syringic acid and vanillic acid were dissolved in sterilized phosphate buffered saline (PBS). Blood was collected from the orbital sinus 24 h after the ConA administration and analyzed for transaminases. The blood was sampled at 24 h because the transaminase levels peaked at 24 h after the ConA treatment. The animal experiments were conducted in accordance with the ethical guidelines of the Osaka University Graduate School of Pharmaceutical Sciences.

Analysis of Liver Enzymes The serum aspartate aminotransferase (AST) and ALT levels were measured by using an assay kit (Transaminase C, WAKO, Osaka, Japan).

Cytokine Determination by ELISA The IL-6, TNF-α, and IFN-γ levels in serum samples were determined by using a mouse enzyme-linked immunosorbent assay (ELISA) kit (Biosource, San Jose, CA, U.S.A.). Analyses were performed according to the manufacturer's instructions. The blood samples were collected at 3, 6, and 9 h because the cytokine levels increased more rapidly than the transaminases and returned to almost normal levels within 12 h.

Histological Analysis Liver specimens were fixed in 4% paraformaldehyde and embedded in paraffin. The tissue blocks were cut into 3-μm sections that were mounted on slides and stained with hematoxylin–eosin.

DPPH Radical-Scavenging Activity The free radical-scavenging activities of L.E.M., syringic acid, and vanillic acid were measured by using the 1,1-diphenyl-2-picrylhdrazyl (DPPH) method.[14] DPPH is a stable free radical that was used for evaluating the scavenging activity by end-point assay. Each compound at the concentration of 0.01 to 1.0 mg/ml was dissolved in ethanol and mixed with DPPH. The reaction was completed within a few minutes. After a 20-min incubation at room temperature in the dark, the absorbance of the sample was read at 517 nm by using a spectrophotometer. The scavenging activity was shown by the decrease in the absorbance at 517 nm.

Preparation of L.E.M. L.E.M. was prepared as previously reported.[15] Briefly, *L. edodes* mycelia were cultivated in solid medium composed of sugarcane bagasse and defatted rice bran. To prepare the culture extract, hot water was added to the medium including the mycelia, and the extract was filtered and lyophilized before being used as the L.E.M. preparation.

Statistics The data were analyzed for statistical significance by the non-parametric Steel–Dwass multiple comparison method. p values less than 0.05 were considered statistically significant.

RESULTS

Effect of L.E.M. on ConA-Induced Liver Injury We examined the hepatoprotective effect of L.E.M. on ConA-induced liver injury in mice. Various amounts of L.E.M. were injected intraperitoneally just before the ConA injection. Twenty-four hours after ConA treatment, the activities of serum AST and ALT were greatly increased as compared to the untreated control (Fig. 1). The intraperitoneal administration of L.E.M. at 20 mg/kg body weight significantly decreased the AST and ALT levels. When administered orally 2 weeks before the ConA treatment, L.E.M. significantly suppressed the increase in transaminases (data not shown).

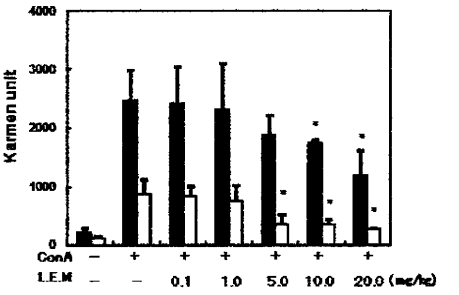

Fig. 1. Effect of L.E.M. on ConA-Induced Liver Injury

Mice received an intravenous injection of ConA (20 mg/kg) and an intraperitoneal injection of L.E.M. (0.1—20 mg/kg). Blood was collected to determine the serum levels of AST (solid columns) and ALT (open columns). The values are the means±S.D. (n=4). *p<0.05 as compared to ConA treatment alone.

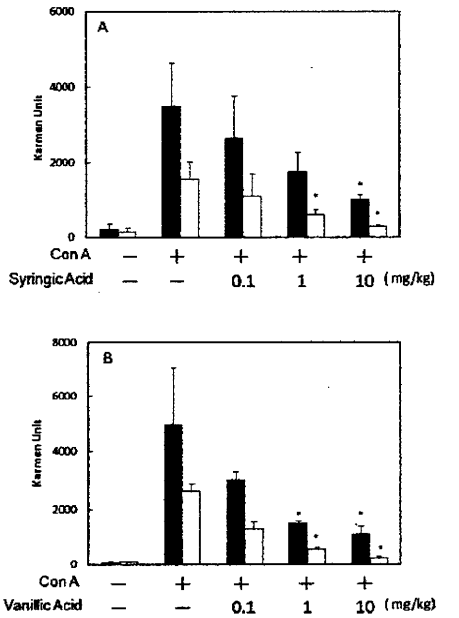

Fig. 2. Effect of Syringic Acid or Vanillic Acid on Transaminase Leakage in ConA-Induced Liver Injury in Mice

Syringic acid (A) or vanillic acid (B) was injected intraperitoneally shortly before the intravenous injection of ConA (20 mg/kg). Blood was collected to measure the serum levels of AST (solid columns) and ALT (open columns). Values are the means±S.D. (n=4). *p<0.05 as compared to the ConA treatment alone.

These results indicate that L.E.M. has a protective effect against ConA-induced liver injury.

Effect of Syringic and Vanillic Acid on ConA-Induced Liver Injury We next examined the hepatoprotective effect of syringic and vanillic acid on the ConA-induced liver injury in mice. Syringic or vanillic acid (0.1, 1.0, or 10.0 mg/kg body weight) was injected intraperitoneally just before the ConA injection. The intraperitoneal administration of syringic or vanillic acid dose-dependently decreased the activities of AST and ALT (Fig. 2). To obtain histological evidence for the protection from liver injury, liver sections were prepared and stained with hematoxylin and eosin; representative images are shown in Fig. 3. The structure of the hepatic sinusoids was normal in the sections from untreated mice. In contrast, the hepatic sinusoids were disorganized and inflammatory infiltration was present in the liver sections from the ConA-treated mice, showing that the liver was injured by the tail-vein injection of ConA. Although some hepatocytes

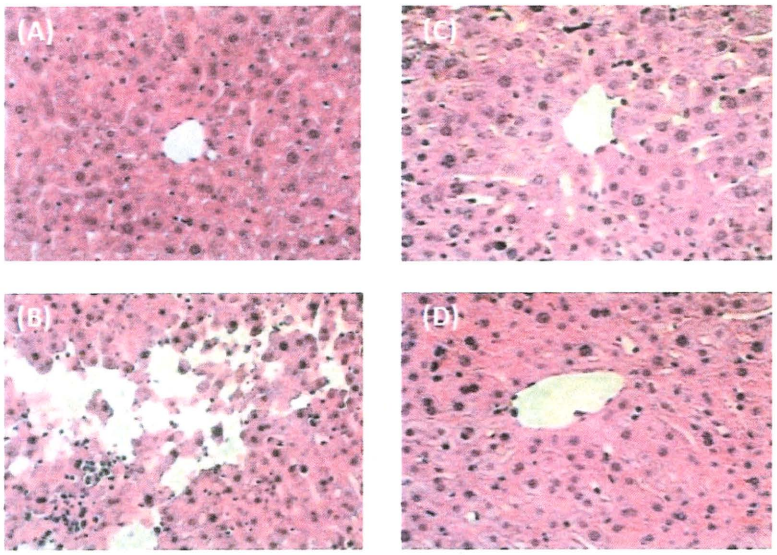

Fig. 3. Suppression of ConA-Induced Liver Injury in Mice That Received Syringic Acid or Vanillic Acid

Sections of paraffin-embedded liver tissue were stained with hematoxylin–eosin. The liver was excised from normal (A), ConA-injured control (B), syringic acid-treated (C), and vanillic acid-treated (D) mice 24 h after ConA injection. Magnification for all photographs, ×400.

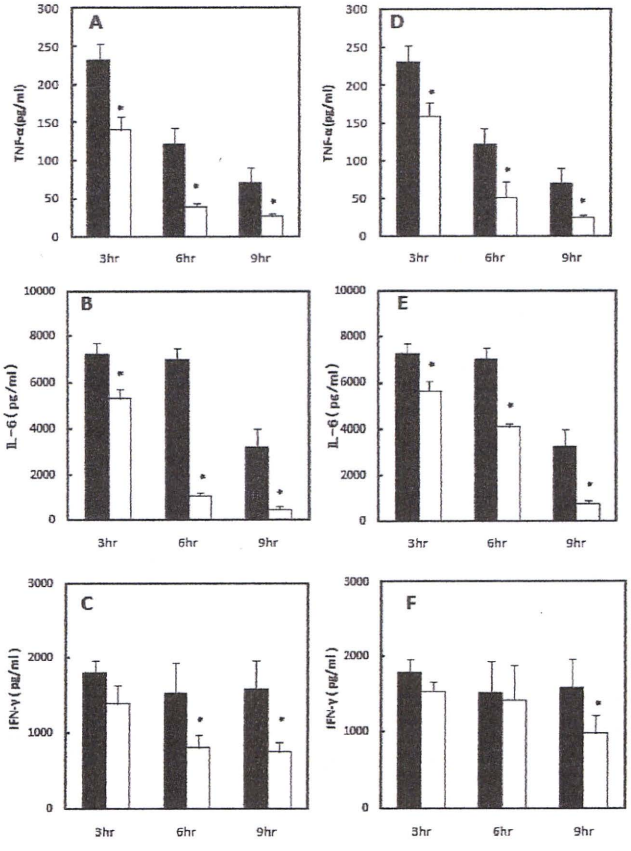

Fig. 4. Changes in Serum TNF-α (A, D), IL-6 (B, E), and IFN-γ (C, F) Levels Measured by ELISA

Mice received an intravenous injection of ConA and intraperitoneal injection of syringic acid (A, B, C) or vanillic acid (D, E, F). Cytokine levels were measured 3, 6, and 9 h after ConA treatment. Solid and open columns indicate the ConA treatment alone and the phenolics treatment, respectively. Values are the means±S.D. (n=4). *p<0.05 as compared to the ConA treatment alone.

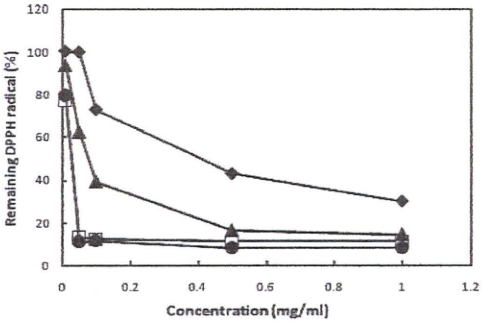

Fig. 5. DPPH Radical-Scavenging Activity of L.E.M., Syringic Acid, and Vanillic Acid

The amount of DPPH radicals was spectrophotometrically determined at 517 nm. Various concentrations of L.E.M. (diamond), syringic acid (open square), and vanillic acid (triangle) were tested. Ascorbic acid (circle) was used as a positive control. Values are the means±S.D. (n=3).

lacking nuclei were seen around the vessel, the disorganization caused by the ConA treatment was decreased in the sections from mice treated with 10 mg/kg of syringic acid or vanillic acid (Figs. 3C, D). Next, we measured the TNF-α, IFN-γ, and IL-6 levels in serum 3, 6, and 9 h after ConA treatment (Fig. 4). The intraperitoneal injection of 10 mg/kg of syringic or vanillic acid significantly decreased the cytokine levels in the serum. These results clearly indicate that syringic acid and vanillic acid have a protective effect against ConA-induced liver injury.

DPPH Radical-Scavenging Activity of L.E.M., Syringic Acid, and Vanillic Acid Figure 5 shows the radical scavenging activities of the samples with DPPH as the substrate. L.E.M. had a dose-dependent scavenging activity that was probably derived from the phenolic compounds including syringic acid and vanillic acid. Both syringic acid and vanillic acid had DPPH radical-scavenging activity; syringic acid had a much higher activity than vanillic acid. This anti-oxidation activity could potentially be effective for suppressing oxidative stress-derived liver injury.

DISCUSSION

This study showed that L.E.M., the hot water extract of cultured mycelia, had a hepatoprotective effect against ConA-induced liver injury in mice, a widely used model of viral hepatitis. Since ConA-induced liver injury is caused by the activation of T cells, the potential immunomodulators contained in the L.E.M., including polysaccharides, glucans, and eritadenine[4,16] could be responsible for the suppressive effect of L.E.M. L.E.M. also contains phenolic compounds that have antioxidation activity, and we previously reported that the administration of L.E.M. suppresses oxidative stress-induced liver injury.[6,7] In the present study, we found that the anti-oxidative phenolic compounds syringic acid and vanillic acid strongly suppressed ConA-induced liver injury in mice.

The physiological functions of plant-derived phenolic compounds have been previously described. Syringic and vanillic acid are reported to possess antimicrobial, anti-cancer, and anti-DNA oxidation activities.[17—19] The present study provides the first evidence that both of these compounds suppress transaminase leakage and inflammatory cytokine production in mice that have ConA-induced liver injury. When these phenolics are orally administered to hamsters, they are absorbed and appear in the plasma within 40 min.[20] Thus, although the phenolics were injected intraperitoneally in the present study, oral administration might also elicit a positive effect on liver injury. Furthermore, these compounds can be obtained in large amounts from inexpensive sources, such as sugarcane molasses. Therefore, syringic and vanillic acid might be promising internal medicines or supplements for suppressing the effects of immune-mediated liver injury, such as the persistent inflammation caused by hepatitis virus infection.

Syringic acid and vanillic acid significantly suppressed the increase in the inflammatory cytokines TNF-α, IFN-γ, and IL-6 elicited *in vivo* by the T-cell mitogen, ConA. Therefore, phenolics might alleviate the uncontrolled immune response through immunomodulation. Sharma *et al.* reported that the plant-derived antioxidant, chlorophyllin, inhibits ConA-induced lymphocyte proliferation *in vitro*.[21] Another antioxidant, resveratrol, is reported to inhibit the production of cytokines, such as IFN-γ and TNF-α, in ConA-treated spleen cells and macrophages.[22] Although chlorophyllin and resveratrol possess various activities that could be responsible for these results, their antioxidation activity could be a major contributor to the suppression of lymphocyte activation. Pani reported that the proliferation of mouse thymocytes in response to ConA treatment is strongly inhibited by the ROS scavenger, *N*-acetylcysteine, and by the inhibitor of NADPH oxidase, diphenyleneiodonium.[23] NADPH oxidase generates ROS after its activation in cells by various types of stimulation.[24] Therefore, the suppressive effect of syringic and vanillic acid on the ConA-induced liver injury might be due to their scavenging of ROS generated by activated NADPH oxidase in the lymphocytes. ConA induces a massive recruitment of activated T cells to the liver. Schwabe reported that ConA-induced liver injury is largely dependent on membrane-bound TNF-α on the infiltrating T cells. The TNF binds to its receptor on hepatocytes to induce ROS production.[24] Syringic acid and vanillic acid could scavenge the ROS to suppress hepatocyte death.

Although syringic and vanillic acids had almost the same effect on liver protection, syringic acid had stronger DPPH activity than vanillic acid. There might be alternative characteristic of these phenolic compounds that are responsible for their liver-protecting effect. Caffeic acid phenethyl ester (CAPE), which is an active phenolic compound contained in propolis, has immunomodulatory and anti-inflammatory properties.[25] Since DNA-binding and transcriptional activities of NF-κB are inhibited in CAPE-treated Jurkat cells, CAPE appears to suppress the proliferation of T cells. Curcumin, a phenolic compound with various biological activities including immunomodulation, suppressed TNF-induced NF-κB-dependent gene transcription.[26] Curcumin and CAPE covalently modify sulfhydryl groups by oxidation and alkylation, and the modification might be responsible for the inhibition of the NF-κB-dependent process. Syringic acid, vanillic acid, and curcumin are phenolic compounds that possess *O*-methoxy groups. Therefore, it is possible that the immunomodulatory effect of syringic and vanillic acids is mediated by inhibiting the NF-κB-dependent process. In the present study, we showed that the cytokine levels were lowered after the administration of syringic acid or vanillic acid in ConA-treated mice; however, the level of suppression was smaller than the anti-inflammatory effect. The inhibition of TNF-induced NF-κB-dependent processes might play an important role in protection against ConA-induced liver injury.

In addition to the ConA-induced acute liver injury, we found that syringic and vanillic acid extensively suppressed the liver fibrosis elicited by chronic treatment with carbon tetrachloride (to be published elsewhere). Thus, these phenolics appear to have physiologically versatile functions. Further studies on the bioavailability, toxicity, and stability of these compounds are underway. The contents of syringic acid and vanillic acid in L.E.M. are 450 and 378 μg/g, respectively. Thus, the contents are relatively small, and the phenolics might not play a major role in immunomodulation effect of L.E.M. However, these phenolics are small molecules that can be easily synthesized in large amounts by organic reactions. These characteristics have clear advantages over immunomodulating glucan or polysaccharide, which seem to be the major components in L.E.M. for drug development.

Acknowledgements We thank the members of our laboratory for their useful comments and discussion.

REFERENCES

1) Gebhardt R., *Planta Med.*, **68**, 289—296 (2002).
2) McKillop I. H., Schrum L. W., *Alcohol*, **35**, 195—203 (2005).
3) Suzuki H., Okubo A., Yamazaki S., Suzuki K., Mitsuya H., Toda S., *Biochem. Biophys. Res. Commun.*, **160**, 367—373 (1989).
4) Yamada T., Oinuma T., Niihashi M., Mitsumata M., Fujioka T., Hasegawa K., Nagaoka H., Itakura H., *J. Atheroscler. Thromb.*, **9**, 149—156 (2002).
5) Yamamoto Y., Shirono H., Kono K., Ohashi Y., *Biosci. Biotechnol. Biochem.*, **61**, 1909—1912 (1997).
6) Akamatsu S., Watanabe A., Tamesada M., Nakamura R., Hayashi S., Kodama D., Kawase M., Yagi K., *Biol. Pharm. Bull.*, **27**, 1957—1960 (2004).
7) Watanabe A., Kobayashi M., Hayashi S., Kodama D., Isoda K., Kondoh M., Kawase M., Tamesada M., Yagi K., *Biol. Pharm. Bull.*, **29**, 1651—1654 (2006).
8) Aggarwal B. B., Kumar A., Bharti A. C., *Anticancer Res.*, **23**, 363—398 (2003).

9) Aviram M., Dornfeld L., Kaplan M., Coleman R., Gaitini D., Nitecki S., Hofman A., Rosenblat M., Volkova N., Presser D., Attias J., Hayek T., Fuhrman B., *Drugs Exp. Clin. Res.*, **28**, 49—62 (2002).
10) Levites Y., Weinreb O., Maor G., Youdim M. B., Mandel S., *J. Neurochem.*, **78**, 1073—1082 (2001).
11) Forrester I. T., Grabski A. C., Mishra C., Kelley B. D., Strickland W. N., Leatham G. F., Burgess R. R., *Appl. Microbiol. Biotechnol.*, **33**, 359—365 (1990).
12) Tiegs G., Hentschel J., Wendel A., *J. Clin. Invest.*, **90**, 196—203 (1992).
13) Cao Q., Batey R., Pang G., Russell A., Clancy R., *Immunol. Cell Biol.*, **76**, 542—549 (1998).
14) Velazquez C., Navarro M., Acosta A., Angulo A., Dominguez Z., Robles R., Robles Zepeda R., Lugo E., Goycoolea F. M., Velazquez E. F., Astiazaran H., Hernandez J., *J. Appl. Microbiol.*, **103**, 1747—1756 (2007).
15) Mizoguchi Y., Katoh H., Kobayashi K., Yamamoto S., Morisawa S., *Gastroenterol. Jpn.*, **22**, 459—464 (1987).
16) Wasser S. P., Weis A. L., *Crit. Rev. Immunol.*, **19**, 65—96 (1999).
17) Aziz N. H., Farag S. E., Mousa L. A., Abo Zaid M. A., *Microbios*, **93**, 43—54 (1998).
18) Guimaraes C. M., Giao M. S., Martinez S. S., Pintado A. I., Pintado M. E., Bento L. S., Malcata F. X., *J. Food Sci.*, **72**, C039—C043 (2007).
19) Kampa M., Alexaki V. I., Notas G., Nifli A. P., Nistikaki A., Hatzoglou A., Bakogeorgou E., Kouimtzoglou E., Blekas G., Boskou D., Gravanis A., Castanas E., *Breast Cancer Res.*, **6**, R63—R74 (2004).
20) Chen C. Y., Milbury P. E., Kwak H. K., Collins F. W., Samuel P., Blumberg J. B., *J. Nutr.*, **134**, 1459—1466 (2004).
21) Sharma D., Kumar S. S., Sainis K. B., *Mol. Immunol.*, **44**, 347—359 (2007).
22) Gao X., Xu Y. X., Janakiraman N., Chapman R. A., Gautam S. C., *Biochem. Pharmacol.*, **62**, 1299—1308 (2001).
23) Pani G., Colavitti R., Borrello S., Galeotti T., *Biochem. J.*, **347 Pt 1**, 173—181 (2000).
24) Bedard K., Krause K. H., *Physiol. Rev.*, **87**, 245—313 (2007).
25) Marquez N., Sancho R., Macho A., Calzado M. A., Fiebich B. L., Munoz E., *J. Pharmacol. Exp. Ther.*, **308**, 993—1001 (2004).
26) Aggarwal S., Ichikawa H., Takada Y., Sandur S. K., Shishodia S., Aggarwal B. B., *Mol. Pharmacol.*, **69**, 195—206 (2006).

European Journal of Pharmaceutics and Biopharmaceutics xxx (2009) xxx–xxx

Contents lists available at ScienceDirect

European Journal of Pharmaceutics and Biopharmaceutics

journal homepage: www.elsevier.com/locate/ejpb

Research paper

Silica nanoparticles as hepatotoxicants

Hikaru Nishimori [a], Masuo Kondoh [a,*], Katsuhiro Isoda [a], Shin-ichi Tsunoda [b,c], Yasuo Tsutsumi [b,c,d], Kiyohito Yagi [a]

[a] Laboratory of Bio-Functional Molecular Chemistry, Graduate School of Pharmaceutical Sciences, Osaka University, Osaka, Japan
[b] Laboratory of Pharmaceutical Proteomics, National Institute of Biomedical Innovation, Osaka, Japan
[c] The Center for Advanced Medicinal Engineering and Informatics, Osaka University, Osaka, Japan
[d] Laboratory of Toxicology, Graduate School of Pharmaceutical Sciences, Osaka University, Osaka, Japan

ARTICLE INFO

Article history:
Received 16 October 2008
Accepted in revised form 9 February 2009
Available online xxxx

Keywords:
Silica particle
Nano-size particle
Liver injury

ABSTRACT

Nano-size materials are increasingly used in cosmetics, diagnosis, imaging and drug delivery, but the toxicity of the nano-size materials has never been fully investigated. Here, we investigated the relationship between particle size and toxicity using silica particles with diameters of 70, 300 and 1000 nm (SP70, SP300, and SP1000) as a model material. To evaluate acute toxicity, we first performed histological analysis of liver, spleen, kidney and lung by intravenous administration of silica particles. SP70-induced liver injury at 30 mg/kg body weight, while SP300 or 1000 had no effect even at 100 mg/kg. Administration of SP70 dose-dependently increased serum markers of liver injury, serum aminotransferase and inflammatory cytokines. Repeated administration of SP70 twice a week for 4 weeks, even at 10 mg/kg, caused hepatic fibrosis. Taken together, nano-size materials may be hepatotoxic, and these findings will be useful for future development in nanotechnology-based drug delivery system.

1. Introduction

The recent development of technology for reducing material size has provided innovative nanomaterials. Nanomaterials are engineered structures with at least one dimension of 100 nm or less, and have unique physicochemical properties with regard to size, chemical composition, surface structure, solubility, shape and aggregation. Nanomaterials have been widely used in microelectronics, catalysts, ultra-sensitive molecular sensing and imaging probes, pharmaceutical agents and cosmetics. Thus, the development of reduced particle size from the macro to the nanoscale provides benefits to a range of industrial and scientific fields. However, materials that are inert in bulk form may be toxic in nano-size forms, and it is thus essential to understand the biological activities and potential toxicity of nanomaterials [1–3].

The influence of inhalation of nanomaterials on human health has been widely investigated. Occupational exposure to quartz, mineral dust particles and asbestos induce inflammation, fibrosis and cytotoxicity in the lung [3]. In animal models, inhaled nanoparticles do not locally remain in the lung, and pass into blood flow, resulting in distribution to distant organs, such as the liver, kidney, brain and heart [4–7]. Moreover, biomedical applications for diagnosis and therapeutic purposes will require intravenous, subcutaneous or intramuscular administration [8–10]. Thus, it is necessary to confirm the influence of nanomaterials in systemic flow on various organs.

Silica nanoparticles have been applied to diagnosis and drug delivery [4,11], and intraperitoneal administration of silica nanoparticles results in the biodistribution of the nanoparticles to diverse organs, such as the liver, kidney, spleen and lung [4]. Both micro- and nano-size silica particles are also commercially available. In the present study, we investigated the influence of nanomaterials on major organs, such as the liver, kidney, spleen and lung using silica particles as a model material. When silica particles with a diameter of 70, 300 or 1000 nm were intravenously injected, only the 70-nm particles led to acute and chronic liver injury.

2. Materials and methods

2.1. Materials

Silica nanoparticles with a diameter of 70, 300 or 1000 nm were purchased from Micromod Partikeltechnologie GmbH (Rostock,

Abbreviations: SP70, 70 nm silica particles; SP300, 300 nm silica particles; SP1000, 1000 nm silica particles; ALT, aminotransferase; BUN, blood urea nitrogen; IL-6, interleukin-6; TNF-α, tumor necrosis factor-α; $GdCl_3$, gadolinium chloride; CPA, cyclophosphamide; LSEC, liver sinusoidal endothelial cells; MARCO, macrophage receptor with collagenous structure.

* Corresponding author. Laboratory of Bio-Functional Molecular Chemistry, Graduate School of Pharmaceutical Sciences, Osaka University, Suita, Osaka 5650871, Japan. Tel.: +81 6 6879 8196; fax: +81 6 6879 8199.
E-mail address: masuo@phs.osaka-u.ac.jp (M. Kondoh).

0939-6411/$ - see front matter © 2009 Elsevier B.V. All rights reserved.
doi:10.1016/j.ejpb.2009.02.005

Germany). The average size of the silica particles was determined to be 75.7, 311 and 830 nm by Zetasizer (Sysmex Co., Kobe, Japan). The particles were spherical and nonporous. The particles were stocked at 25 mg/ml (70 nm) and 50 mg/ml (300 and 1000 nm) in aqueous suspension. The stock solutions were suspended using vortex mixer for 5 min before use. The resultant solutions did not show aggregation of the particles by electron microscopy analysis. Reagents used in this study were of research grade.

2.2. Animals

BALB/c male mice (8 wk) were obtained from Shimizu Laboratory Supplies Co., Ltd. (Kyoto, Japan), and were housed in an environmentally controlled room at 23 ± 1.5 °C with a 12-h light/12-h dark cycle. Mice had free access to water and commercial chow (Type MF, Oriental Yeast, Tokyo, Japan). Mice were intravenously injected with the silica particles at 10–100 mg/kg body weight. The experimental protocols conformed to the ethical guidelines of the Graduate School of Pharmaceutical Sciences, Osaka University.

2.3. Histological analysis

The liver, kidney, spleen and lung were removed and fixed with 4% paraformaldehyde. After sectioning, thin tissue sections of tissues were stained with hematoxylin and eosin for histological observation. Liver sections were stained with Azan-Mallory for observation of liver fibrosis.

2.4. Biochemical assay

Serum alanine aminotransferase (ALT) levels and blood urea nitrogen (BUN) were measured using a commercially available Transaminase-CII kit and Blood Urea Nitrogen-B Test Wako (WAKO Pure Chemical, Osaka, Japan), respectively. Interleukin-6 (IL-6) and tumor necrosis factor-α (TNF-α) were measured with an ELISA kit (BioSource International, CA, USA).

2.5. Gadolinium chloride assay

For Kupffer cell blockage of phagocytosis and partial depletion in the liver, mice were injected intravenously with gadolinium chloride ($GdCl_3$) at 10 mg/kg body weight at 30 and 6 h prior to intravenous administration of nanoparticles [12,13]. Blood was then recovered 24 h after injection of nanoparticles for ALT assay.

2.6. Cyclophosphamide assay

Disruption of liver sinusoidal endothelial cells was carried out by intraperitoneal injection of 300 mg/kg body weight cyclophosphamide (CPA) at 24 h prior to administration of nanoparticles [14,15]. Blood was recovered at 24 h after injection of nanoparticles for ALT assay.

2.7. Hepatic hydroxyproline content

Hepatic hydroxyproline content was assayed by Kivirikko's method, with some modification [16]. Briefly, liver tissue was hydrolyzed in 6 M HCl at 110 °C for 24 h in a glass tube. After centrifugation, the resultant supernatant was neutralized with 8 N KOH, and 2 g of KCl and 1 ml of 0.5 M borate buffer were then added, followed by incubation for 15 min at room temperature and further incubation for 15 min at 0 °C. Chloramine-T solution was then prepared and added. After additional incubation for 1 h at 0 °C, 2 ml of 3.6 M sodium thiosulfate was added, followed by incubation at 120 °C for 30 min. Next, 3 ml of toluene was added with incubation for a further 20 min at room temperature. After centrifugation, 2 ml of the resultant supernatant was added to Ehrlich's reagent, followed by incubation for 30 min at room temperature. Subsequently, the absorbance was measured at 560 nm.

2.8. Statistical analysis

Statistical analysis was performed by two-way ANOVA, followed by Student's *t*-test. The level of significance was set at $p < 0.05$.

3. Results

3.1. Liver injury by 70-nm silica nanoparticles

We initially investigated the acute toxicity of silica particles with diameters of 70 (SP70), 300 (SP300) or 1000 nm (SP1000) at maximal dose of 100 mg/kg. Intravenous injection of SP70 at 50 and 100 mg/kg was often lethal, but mice injected with SP300 and SP1000 survived. Fig. 1 shows hematoxylin–eosin staining of the liver, spleen, lung and kidney in silica particle-injected mice. We found no toxicity in any of these organs in SP300 or SP1000-injected mice at 100 mg/kg, and we found no abnormalities in the spleen, kidney and lung in SP70-injected mice at 30 mg/kg (Fig. 1A–D). However, degenerative necrosis of hepatocytes in the liver was observed in SP70-injected mice, thus suggesting that SP70 is toxic to the liver (Fig. 1A).

Next, in order to confirm the hepatotoxicity of SP70, we examined serum ALT activity, a biochemical marker of liver injury. Consistent with the histological data, injection of SP70 elevated serum ALT levels 35-fold over control values at 30 mg/kg, but injection of SP300 or SP1000 had no effect even at 100 mg/kg (Fig. 2A). Elevation of blood urea nitrogen, a biochemical marker of kidney injury, was not observed (Fig. 2B). Serum levels of inflammatory cytokine IL-6 and TNF-α were markedly elevated to 1124 and 80 pg/ml, respectively, in SP70-treated mice at 3 h (Fig. 2B and C). Slight elevation of serum IL-6 levels was observed in SP300- and SP1000-injected mice (28 and 32 pg/ml, respectively), while no elevation of TNF-α was observed. The IL-6 levels seen in SP300- or SP1000-treated mice were insufficient for liver injury. To investigate dose dependency of SP70-induced liver injury, we also investigated serum ALT and inflammatory cytokine levels at 12 h after SP70 administration. ALT, IL-6 and TNF-α levels were elevated in a dose-dependent manner after SP70 injection, and significant increases were observed with doses as low as 20 mg/kg (Fig. 3A–C). Taken together, these data suggest that 70-nm silica particles are toxic to the liver.

3.2. Involvement of Kupffer cells in SP70-induced liver injury

Kupffer cells are large liver macrophages, and are localized within the liver sinusoidal cells. Kupffer cells play a role in defense against various particles and substances entering the liver through the portal circulation [17]. Indeed, Kupffer cells clear virus particles from the bloodstream by phagocytosis [18–20]. The phagocytosis of parasites by Kupffer cells is accompanied by the release of proinflammatory cytokines that act as a paracrine signal to neighboring hepatocytes, and induce chemotaxis and aggregation of neutrophils. $GdCl_3$ inhibits phagocytosis by Kupffer cells and transiently eliminates Kupffer cells [12], and $GdCl_3$ has thus been widely used to investigate the roles of Kupffer cells in the liver [21,22]. To investigate the involvement of Kupffer cells in particle-induced liver injury, we evaluated the effects of $GdCl_3$ on nanoparticle-induced liver injury. As shown in Fig. 4A, pre-injection of $GdCl_3$ prior to injection of SP70 elevated serum ALT levels 5.5-fold

Please cite this article in press as: H. Nishimori et al., Silica nanoparticles as hepatotoxicants, Eur. J. Pharm. Biopharm. (2009), doi:10.1016/j.ejpb.2009.02.005

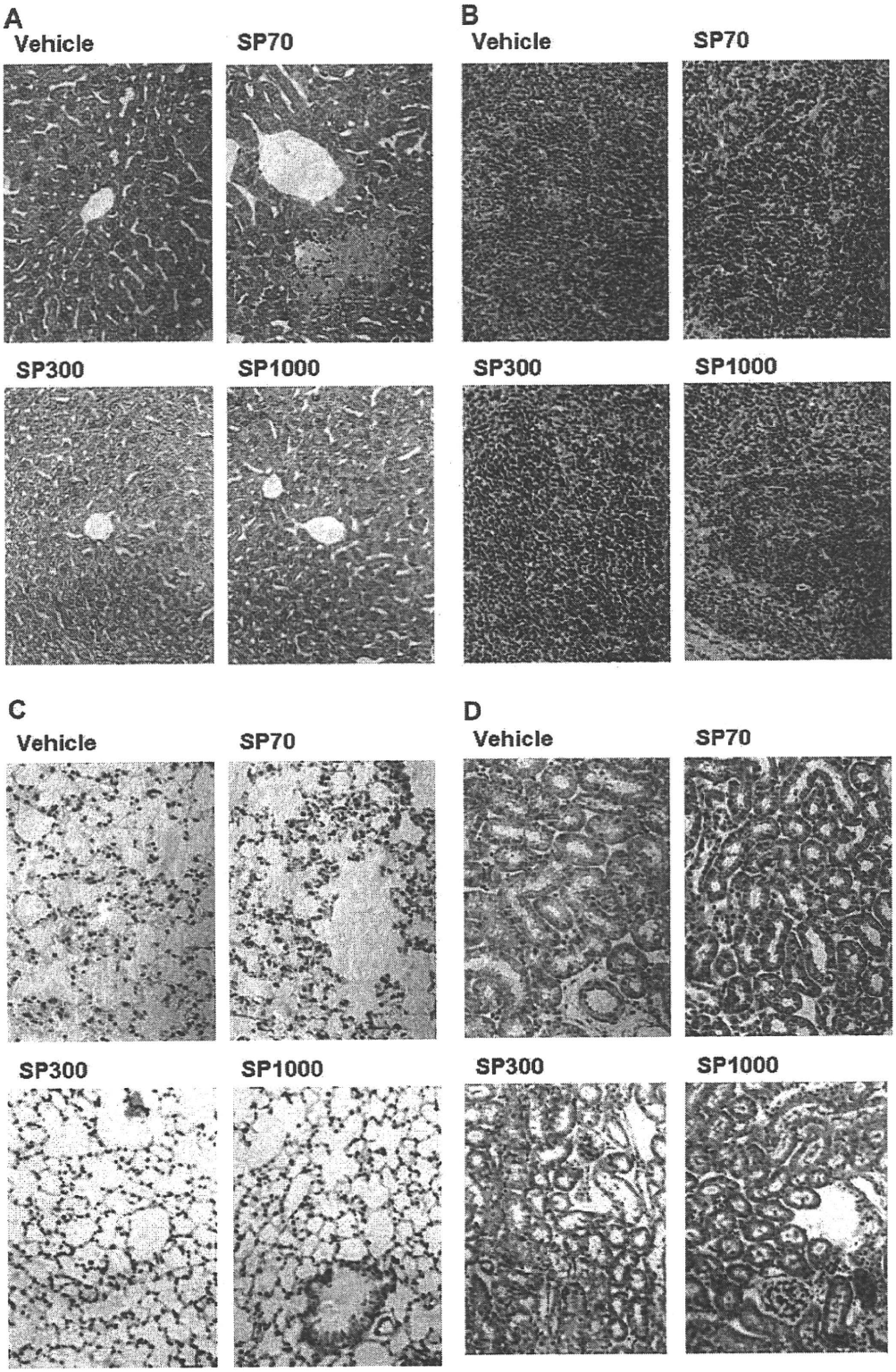

Fig. 1. Histological analysis of tissues in silica particle-treated mice. Silica particles with diameters of 70 (SP70), 300 (SP300) or 1000 nm (SP1000) were intravenously administered to mice at 30, 100 and 100 mg/kg, respectively. At 24 h after administration, tissues of liver (A), spleen (B), lung (C) and kidney (D) were collected, and fixed with 4% paraformaldehyde. Tissue sections were stained with hematoxylin and eosin and observed under a microscope. Data are representative of at least four mice.

in the SP70-injected group. In contrast, pre-injection of $GdCl_3$ did not affect ALT levels in the SP300- or SP1000-administered group. Taken together, these results indicate that phagocytosis of SP70 by Kupffer cells may attenuate liver injury, but the release of proinflammatory cytokines from Kupffer cells is not associated with SP70-induced liver injury.

Please cite this article in press as: H. Nishimori et al., Silica nanoparticles as hepatotoxicants, Eur. J. Pharm. Biopharm. (2009), doi:10.1016/j.ejpb.2009.02.005

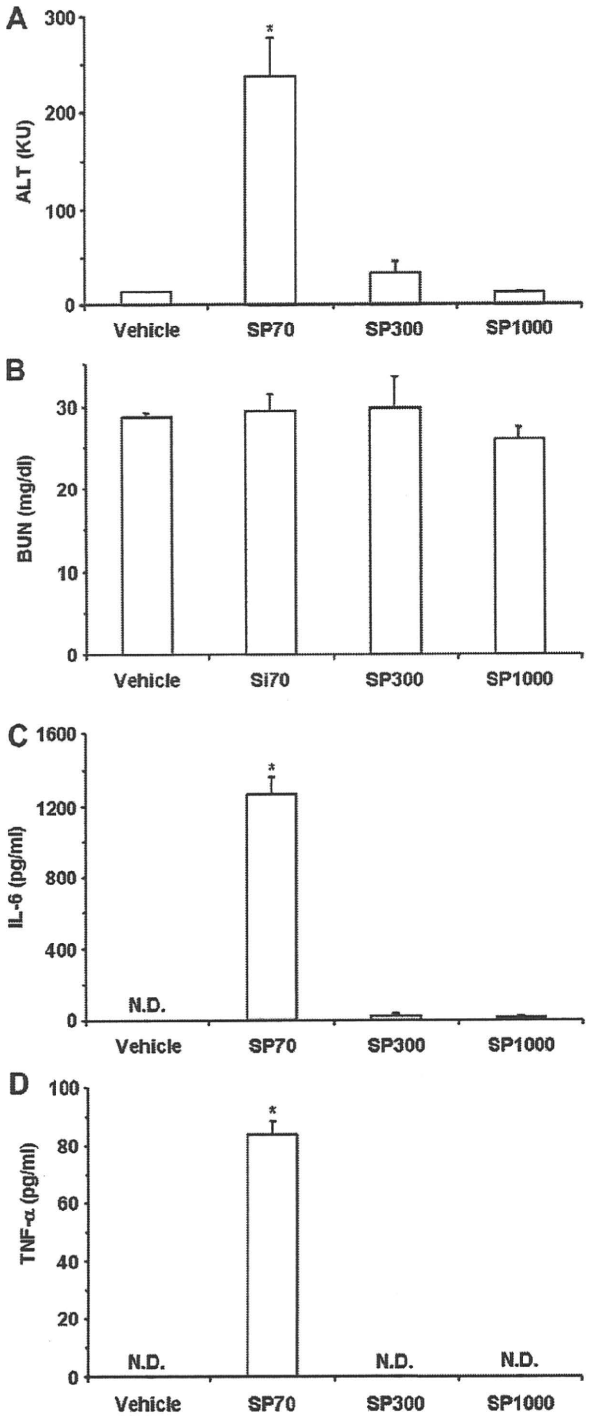

Fig. 2. Biochemical analyses of liver injury in silica particle-injected mice. SP70, SP300 or SP1000 was intravenously injected to mice at 30, 100 or 100 mg/kg, respectively. Blood was recovered at 3 and 24 h of the injection. Serum ALT (A) and BUN (B) at 24 h and IL-6 (C) and TNF-α (D) levels at 3 h were measured using a commercially available kit, as described in Section 2. Data are means ± SEM ($n = 4$). *Significant difference vs. vehicle-treated group ($p < 0.05$).

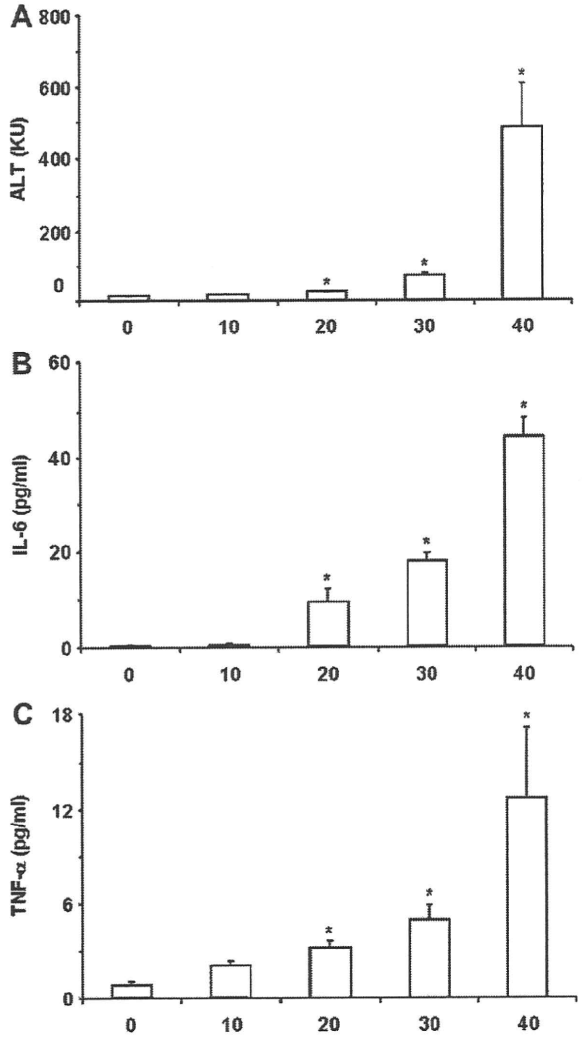

Fig. 3. Dose dependency of SP70 on liver injury. SP70 were intravenously administered at the indicated doses, and blood was recovered at 12 h after administration. Serum was used for measurement of ALT (A), IL-6 (B) and TNF-α (C), as described in Section 2. Data are means ± SEM ($n = 4$). *Significant difference compared with the vehicle-treated group ($p < 0.05$).

3.3. Involvement of liver sinusoidal endothelial cells in SP70-induced liver injury

Sinusoidal endothelium forms a barrier between the bloodstream and hepatocytes, preventing passage of particles. Liver sinusoidal endothelial cells (LSECs) are perforated by fenestrations, which are pores of approximately 100 nm in diameter. SP70, but not SP300 and SP1000, may pass through LSECs to the hepatocytes, resulting in liver injury. To evaluate this hypothesis, we performed CPA assay. CPA is converted in the liver to toxic metabolites, 4-hydroperoxycyclophosphamide and acrolein, to which endothelial cells are 20-fold more susceptible than hepatocytes [14]. CPA has been shown to disrupt LSECs [14,15]. We thus investigated the effects of CPA on nanoparticle-induced liver injury. As shown in Fig. 4B, pre-injection of CPA did not affect ALT levels in SP300- or SP1000-administered mice, whereas CPA dramatically decreased ALT levels to near control values in SP70-injected mice (from 235 to 29 KU). These data on CPA indicate that LSECs may be directly or indirectly involved in SP70-induced liver injury, but may not be a barrier against SP70.

3.4. Chronic toxicity of SP70

Finally, we investigated the effects of SP70 on chronic liver injury. SP70 was injected into mice every 3 days for 4 weeks at 10 or 30 mg/kg. The lower dose (10 mg/kg) did not cause acute liver

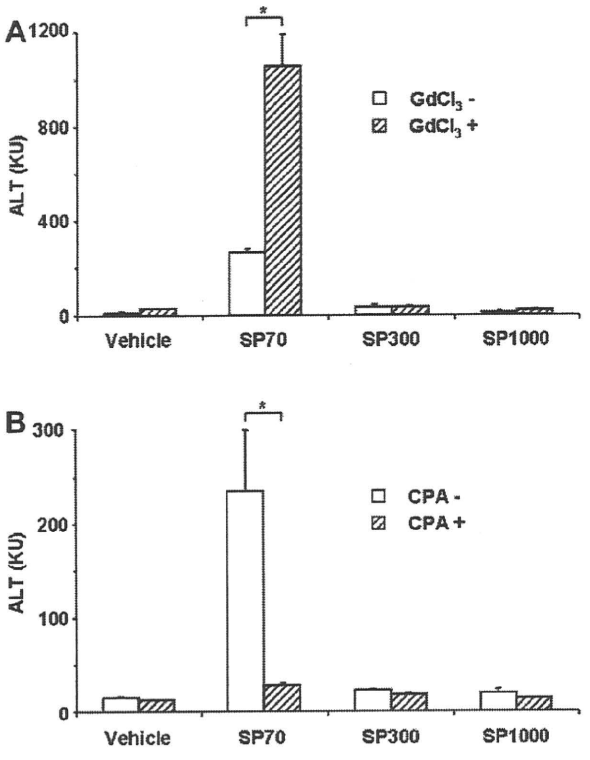

Fig. 4. Pharmaceutical analysis of SP70-induced liver injury. (A) $GdCl_3$ assay. Vehicle or $GdCl_3$ (10 mg/kg) was intravenously injected into mice at 30 h or 6 h prior to treatment with silica particles (SP70, 30 mg/kg; SP300, 100 mg/kg; SP1000, 100 mg/kg). At 24 h after particle administration, blood was recovered, and the resultant serum was used for ALT assay. Data are means ± SEM ($n = 4$). *Significant difference between vehicle- and silica particle-treated groups ($p < 0.05$). (B) CPA assay. Vehicle or CPA (300 mg/kg) was intraperitoneally injected to mice at 24 h prior to treatment with silica particles. At 24 h after administration of particles, blood was recovered, and the resultant serum was used for ALT assay. Data are means ± SEM ($n = 4$). *Significant difference between vehicle- and silica particle-treated groups ($p < 0.05$).

failure (Fig. 3A). Histological analysis demonstrated that chronic exposure of SP70-induced denaturation of hepatocytes in a dose-dependent manner (Fig. 5A). Serum ALT levels were also elevated by SP70 administration (Vehicle, 14.3 KU; SP70, 24.8 and 42.1 KU at 10 and 30 mg/kg, respectively) (Fig. 5B). Liver fibrosis is a symptom of chronic liver injury, and thus, we investigated liver fibrosis. Collagen, which is accumulated in the fibrotic liver, was stained with Azan reagent, and blue-stained regions were observed in SP70-treated, but not vehicle-treated, liver sections (Fig. 5C). Elevated hydroxyproline content parallels the extent of fibrosis, and we investigated the hydroxyproline contents in the SP70-treated mouse liver. Injection of SP70 significantly elevated hepatic hydroxyproline contents 1.6- and 3.5-fold over control values, at 10 mg/kg and 30 mg/kg, respectively (Fig. 5D). These data indicate that chronic administration of SP70 causes liver fibrosis, even at doses that are non-toxic in a single injection.

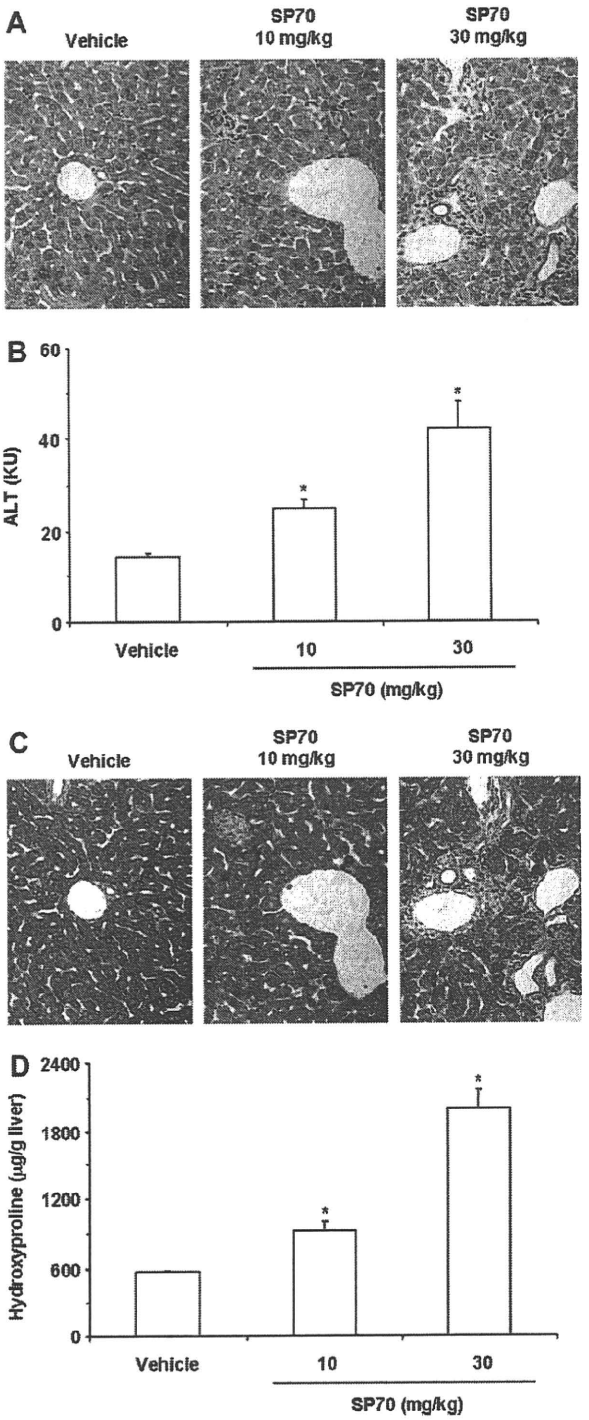

Fig. 5. Effect of SP70 on chronic liver injury. Mice were subjected to repeated administration of SP70 (10 or 30 mg/kg) every 3 days for 4 weeks. At 3 days after the last administration, mice were sacrificed. Tissues of livers were fixed with 4% paraformaldehyde, and liver sections were then stained with hematoxylin and eosin (A) or Azan (C). Hydroxyproline levels in the liver were assayed as described in Section 2 (C). Serum samples were used for measurement of ALT (B). (A and C) Data are representative of at least eight mice. (B) Data are means ± SEM ($n = 4$). *Significant difference vs. vehicle-treated group ($p < 0.05$).

4. Discussion

In the present study, we evaluated the acute toxicity of silica particles with a diameter of 70, 300 or 1000 nm, and we found that 70-nm silica particles injure the liver, but not the spleen, lung or kidney. Moreover, chronic administration of 70-nm silica particles caused liver fibrosis, even at doses that were non-toxic in a single injection.

Surface area is a critical factor for toxicity of nano-size particles in the liver. The numbers of particles of SP70, 300 and 1000 are 2.8×10^{12}, 3.5×10^{10} and 9.5×10^{8} particles/mg, respectively. The surface area of SP300 at 100 mg/kg, at which SP300 was not toxic, is similar to that of SP70 at 30 mg/kg, at which SP70 was toxic. Difference in the surface area may not affect the different toxicities in the liver between SP70 and 300.

Please cite this article in press as: H. Nishimori et al., Silica nanoparticles as hepatotoxicants, Eur. J. Pharm. Biopharm. (2009), doi:10.1016/j.ejpb.2009.02.005

There are highly specialized endothelial cells, LSECs, in the liver, and these separate sinusoidal blood from hepatocytes. Passage of particles through LSECs is the first step for translocation from the bloodstream to hepatocytes. LSECs have fenestrations with a diameter of 100 nm, and the liver injury seen with 70-nm silica particles may be due to the particle size. We investigated the role of LSECs in the particle-induced liver injury using CPA, a disruptor of LSECs [13–15]. Unexpectedly, the disruption of LSEC did not cause SP300- and SP1000-induced liver injury. These results were consistent with the previous report that disruption of LSECs by CPA did not affect the hepatocyte transduction of a lentivirus vector with a diameter of 120–200 nm larger than the fenestrations of LSECs [13]. In contrast, SP70-induced liver injury was dramatically suppressed by disruption of LSECs, and pores in the LSEC may be responsible for the hepatic toxicity of SP70. Spaces, called the space of Disse, exist between LSEC and hepatocytes [23]. Particles entering into these spaces can avoid efflux into the blood flow in the sinusoids of the liver, resulting that this may enhance interaction between the particles and hepatocytes. Thus, the Disse spaces between LSECs and hepatocytes may be responsible for the liver injury caused by SP70.

Resident macrophages in the liver, Kupffer cells play a pivotal role in defense against foreign particles by eliminating such particles via phagocytosis [17]. $GdCl_3$ has been widely used to block phagocytosis by Kupffer cells and to deplete Kupffer cells [12,13,20,21]. Inactivation of Kupffer cells had no effect on SP300 and SP1000 treatment, whereas pre-treatment with $GdCl_3$ led to increased liver injury by SP70. There is no evidence that $GdCl_3$ exerts any direct toxic effects on hepatocytes, LSECs, or on other cells in the liver [24]. Thus, the elevation of SP70 toxicity may be caused by the depletion of Kupffer cells. Depletion of Kupffer cells enhanced the transgene activity of adenovirus vectors with a similar size with SP70 in the liver [22]. Therefore, inhibition of phagocytosis of Kupffer cells may enhance the interaction between SP70 and hepatocytes by increase in SP70 moving into the Disse spaces. Inhalation of silica particles causes lung injury [25], and alveolar macrophages function as a defense against inhaled agents, including viruses and environmental particles, via phagocytosis [26]. Macrophage receptor with collagenous structure (MARCO), CD204 and CD36 are reported to be the receptors for inert particles [26–30]. Uptake of silica particles through MARCO or CD204 induces cytotoxicity in alveolar macrophages, leading to lung fibrosis [30,31]. Alveolar macrophages from BALB/c do not express MARCO and CD204, and silica particles are taken up through CD36 [30]. Thus, uptake of SP70 by Kupffer cells through CD36 might not trigger liver injury. In this study, we found that chronic administration of SP70 caused liver fibrosis, even at 10 mg/kg body weight, at which level acute liver injury was not observed after a single injection. Nano-size particles-induced continuous inflammation in the liver will cause liver fibrosis leading to hepatic cancer.

Further evaluation of relationship between toxicity and variety of sizes, shapes, and chemical modification on the surface of particles is needed, and the future studies based on these data will provide very useful information on future development of drug delivery system using nano-size materials.

Acknowledgements

The authors thank all members of our laboratory for their useful comments and discussion. This study was supported by a grant from the Ministry of Health, Labor, and Welfare of Japan.

References

[1] R.F. Service, U.S. nanotechnology. Health and safety research slated for sizable gains, Science 315 (2007) 926.
[2] A. Nel, T. Xia, L. Madler, N. Li, Toxic potential of materials at the nanolevel, Science 311 (2006) 622–627.
[3] G. Oberdorster, E. Oberdorster, J. Oberdorster, Nanotoxicology: an emerging discipline evolving from studies of ultrafine particles, Environ. Health Perspect. 113 (2005) 823–839.
[4] J.S. Kim, T.J. Yoon, K.N. Yu, B.G. Kim, S.J. Park, H.W. Kim, K.H. Lee, S.B. Park, J.K. Lee, M.H. Cho, Toxicity and tissue distribution of magnetic nanoparticles in mice, Toxicol. Sci. 89 (2006) 338–347.
[5] S. Takenaka, E. Karg, C. Roth, H. Schulz, A. Ziesenis, U. Heinzmann, P. Schramel, J. Heyder, Pulmonary and systemic distribution of inhaled ultrafine silver particles in rats, Environ. Health Perspect. 109 (Suppl. 4) (2001) 547–551.
[6] A. Nemmar, P.H. Hoet, B. Vanquickenborne, D. Dinsdale, M. Thomeer, M.F. Hoylaerts, H. Vanbilloen, L. Mortelmans, B. Nemery, Passage of inhaled particles into the blood circulation in humans, Circulation 105 (2002) 411–414.
[7] A. Nemmar, H. Vanbilloen, M.F. Hoylaerts, P.H. Hoet, A. Verbruggen, B. Nemery, Passage of intratracheally instilled ultrafine particles from the lung into the systemic circulation in hamster, Am. J. Respir. Crit. Care Med. 164 (2001) 1665–1668.
[8] M. Vallet-Regi, F. Balas, D. Arcos, Mesoporous materials for drug delivery, Angew. Chem. Int. Ed. Engl. 46 (2007) 7548–7558.
[9] S.D. Caruthers, S.A. Wickline, G.M. Lanza, Nanotechnological applications in medicine, Curr. Opin. Biotechnol. 18 (2007) 26–30.
[10] Z. Medarova, W. Pham, C. Farrar, V. Petkova, A. Moore, In vivo imaging of siRNA delivery and silencing in tumors, Nat. Med. 13 (2007) 372–377.
[11] M. Bottini, F. D'Annibale, A. Magrini, F. Cerignoli, Y. Arimura, M.I. Dawson, E. Bergamaschi, N. Rosato, A. Bergamaschi, T. Mustelin, Quantum dot-doped silica nanoparticles as probes for targeting of T-lymphocytes, Int. J. Nanomed. 2 (2007) 227–233.
[12] M.J. Hardonk, F.W. Dijkhuis, C.E. Hulstaert, J. Koudstaal, Heterogeneity of rat liver and spleen macrophages in gadolinium chloride-induced elimination and repopulation, J. Leukoc. Biol. 52 (1992) 296–302.
[13] N.P. van Til, D.M. Markusic, R. van der Rijt, C. Kunne, J.K. Hiralall, H. Vreeling, W.M. Frederiks, R.P. Oude-Elferink, J. Seppen, Kupffer cells and not liver sinusoidal endothelial cells prevent lentiviral transduction of hepatocytes, Mol. Ther. 11 (2005) 26–34.
[14] L.D. DeLeve, Cellular target of cyclophosphamide toxicity in the murine liver: role of glutathione and site of metabolic activation, Hepatology 24 (1996) 830–837.
[15] H. Malhi, P. Annamaneni, S. Slehria, B. Joseph, K.K. Bhargava, C.J. Palestro, P.M. Novikoff, S. Gupta, Cyclophosphamide disrupts hepatic sinusoidal endothelium and improves transplanted cell engraftment in rat liver, Hepatology 36 (2002) 112–121.
[16] K.I. Kivirikko, O. Laitinen, D.J. Prockop, Modifications of a specific assay for hydroxyproline in urine, Anal. Biochem. 19 (1967) 249–255.
[17] K. Decker, Biologically active products of stimulated liver macrophages (Kupffer cells), Eur. J. Biochem. 192 (1990) 245–261.
[18] K.T. Brunner, D. Hurez, C.R. Mc, B. Benacerraf, Blood clearance of P32-labeled vesicular stomatitis and Newcastle disease viruses by the reticuloendothelial system in mice, J. Immunol. 85 (1960) 99–105.
[19] L. Zhang, P.J. Dailey, A. Gettie, J. Blanchard, D.D. Ho, The liver is a major organ for clearing simian immunodeficiency virus in rhesus monkeys, J. Virol. 76 (2002) 5271–5273.
[20] R. Alemany, K. Suzuki, D.T. Curiel, Blood clearance rates of adenovirus type 5 in mice, J. Gen. Virol. 81 (2000) 2605–2609.
[21] A. Lieber, C.Y. He, L. Meuse, D. Schowalter, I. Kirillova, B. Winther, M.A. Kay, The role of Kupffer cell activation and viral gene expression in early liver toxicity after infusion of recombinant adenovirus vectors, J. Virol. 71 (1997) 8798–8807.
[22] G. Schiedner, S. Hertel, M. Johnston, V. Dries, N. van Rooijen, S. Kochanek, Selective depletion or blockade of Kupffer cells leads to enhanced and prolonged hepatic transgene expression using high-capacity adenoviral vectors, Mol. Ther. 7 (2003) 35–43.
[23] E. Wisse, R.B. De Zanger, K. Charels, P. Van Der Smissen, R.S. McCuskey, The liver sieve: considerations concerning the structure and function of endothelial fenestrae, the sinusoidal wall and the space of Disse, Hepatology 5 (1985) 683–692.
[24] R.M. Rai, S.Q. Yang, C. McClain, C.L. Karp, A.S. Klein, A.M. Diehl, Kupffer cell depletion by gadolinium chloride enhances liver regeneration after partial hepatectomy in rats, Am. J. Physiol. 270 (1996) G909–918.
[25] G.S. Cooper, F.W. Miller, D.R. Germolec, Occupational exposures and autoimmune diseases, Int. Immunopharmacol. 2 (2002) 303–313.
[26] M. Arredouani, Z. Yang, Y. Ning, G. Qin, R. Soininen, K. Tryggvason, L. Kobzik, The scavenger receptor MARCO is required for lung defense against pneumococcal pneumonia and inhaled particles, J. Exp. Med. 200 (2004) 267–272.
[27] L. Kobzik, Lung macrophage uptake of unopsonized environmental particulates. Role of scavenger-type receptors, J. Immunol. 155 (1995) 367–376.
[28] M.S. Arredouani, A. Palecanda, H. Koziel, Y.C. Huang, A. Imrich, T.H. Sulahian, Y.Y. Ning, Z. Yang, T. Pikkarainen, M. Sankala, S.O. Vargas, M. Takeya, K. Tryggvason, L. Kobzik, MARCO is the major binding receptor for unopsonized particles and bacteria on human alveolar macrophages, J. Immunol. 175 (2005) 6058–6064.
[29] A. Palecanda, J. Paulauskis, E. Al-Mutairi, A. Imrich, G. Qin, H. Suzuki, T. Kodama, K. Tryggvason, H. Koziel, L. Kobzik, Role of the scavenger receptor MARCO in alveolar macrophage binding of unopsonized environmental particles, J. Exp. Med. 189 (1999) 1497–1506.
[30] R.F. Hamilton Jr., S.A. Thakur, J.K. Mayfair, A. Holian, MARCO mediates silica uptake and toxicity in alveolar macrophages from C57BL/6 mice, J. Biol. Chem. 281 (2006) 34218–34226.
[31] R.F. Hamilton Jr., S.A. Thakur, A. Holian, Silica binding and toxicity in alveolarmacrophages, Free Radic. Biol. Med. 44 (2008) 1246–1258.

Please cite this article in press as: H. Nishimori et al., Silica nanoparticles as hepatotoxicants, Eur. J. Pharm. Biopharm. (2009), doi:10.1016/j.ejpb.2009.02.005